https://doi.org/10.25923/v03z-gc36

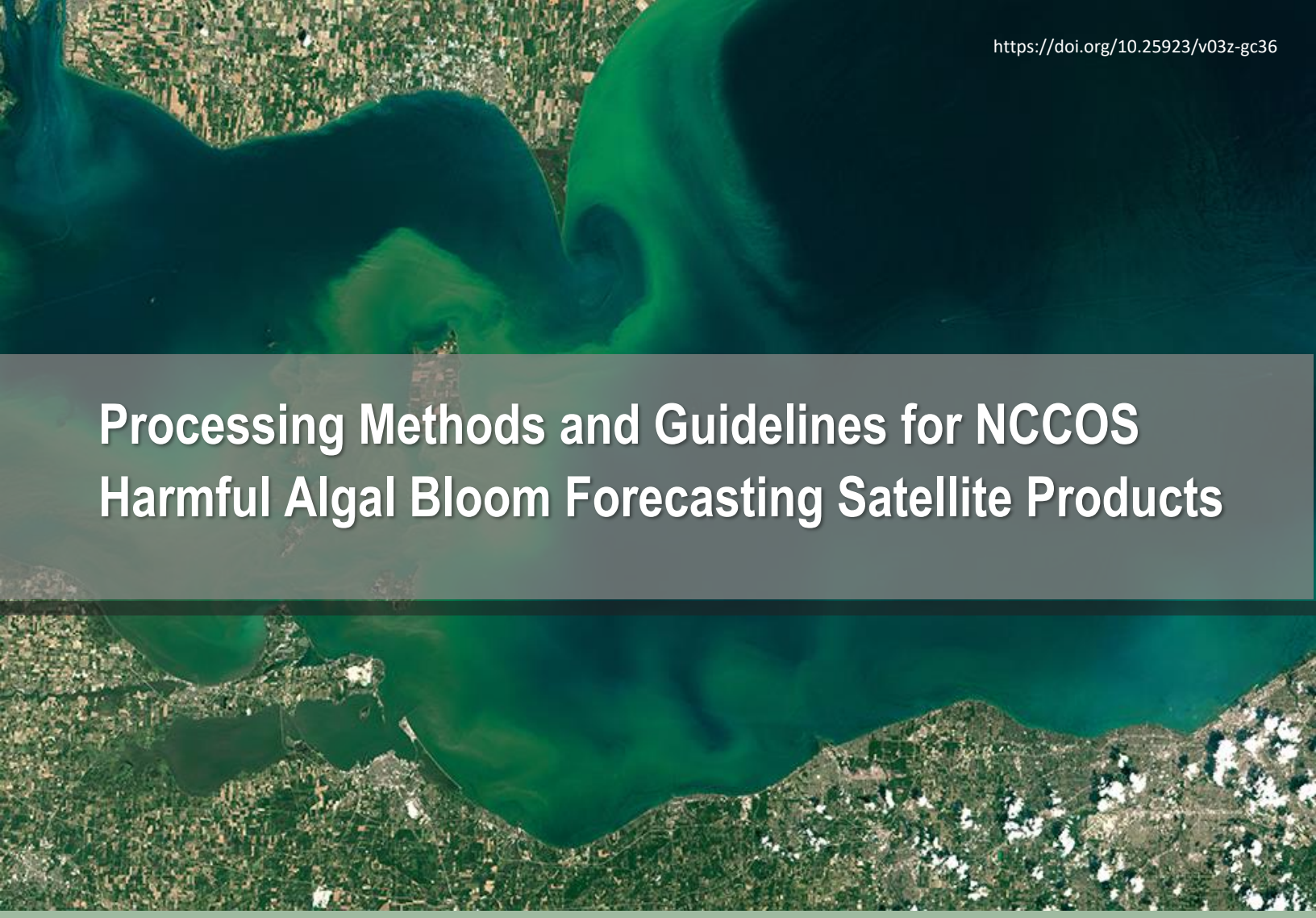

Processing Methods and Guidelines for NCCOS Harmful Algal Bloom Forecasting Satellite Products

Authors

Timothy T. Wynne
Andrew Meredith
Sachidananda Mishra
Kari St. Laurent
Richard P. Stumpf

January 2026

NOAA TECHNICAL MEMORANDUM NOS NCCOS 366

NOAA NCCOS Harmful Algal Bloom Forecasting Branch

National Centers for Coastal Ocean Science
NOAA National Ocean Service
U.S. Department of Commerce

SUGGESTED CITATION

Wynne, T. T., Meredith, A., Mishra, S., St. Laurent, K., and Stumpf, R. (2026). Processing methods and guidelines for NCCOS harmful algal bloom forecasting satellite products. NOAA Technical Memorandum NOS NCCOS 366.
https://doi.org/10.25923/v03z-gc36

ACKNOWLEDGMENTS

The authors would like to thank Alexandria Hounshell and Michelle Tomlinson for their insightful reviews and constructive feedback throughout the development of this document. Their expertise and careful review helped improve the technical content and clarity of the memo. The authors also acknowledge Bridget Weimer for formatting and document preparation, as well as additional reviewers and NCCOS leadership for their time and contributions to the review process.

For more information, please contact:
Timothy Wynne, PhD
timothy.wynne@noaa.gov
or
hab@noaa.gov

PHOTOGRAPHY

NOAA National Centers for Coastal Ocean Science. Image derived from MODIS satellite observations.

Processing Methods and Guidelines for NCCOS Harmful Algal Bloom Forecasting Satellite Products

Prepared by

NOAA National Ocean Service
National Centers for Coastal Ocean Science
Stressor Detection and Impacts Division
Harmful Algal Bloom Forecasting Branch
Silver Spring, MD

Authors

Timothy T. Wynne[1,2], Andrew Meredith[3,4], Sachidananda Mishra[3,5], Kari St. Laurent[1,6], and Richard Stumpf[1,7]

[1] *NOAA, National Ocean Service, National Centers for Coastal Ocean Science*
[2] *https://orcid.org/0000-0001-7282-0866*
[3] *CSS, Inc., under contract to NOAA, National Ocean Service, National Centers for Coastal Ocean Science*
[4] *https://orcid.org/0000-0001-9651-7132*
[5] *https://orcid.org/0000-0001-6613-3103*
[6] *https://orcid.org/0000-0001-9797-0190*
[7] *https://orcid.org/0000-0001-5531-6860*

January 2026

NOAA TECHNICAL MEMORANDUM NOS NCCOS 366

Table of Contents

List of Figures

List of Tables

Executive Summary

The NOAA National Centers for Coastal Ocean Science (NCCOS) Harmful Algal Bloom Forecasting Branch (HAB-F) develops and maintains an operational suite of satellite ocean-color products to support the detection, monitoring, and forecasting of harmful algal blooms (HABs) in U.S. coastal and inland waters. Satellite remote sensing provides the only practical means of delivering synoptic, repeatable observations across large spatial domains, making it a foundational component of the National Oceanic and Atmospheric Administration's (NOAA) HAB monitoring and forecast enterprise.

This document provides a consolidated and updated description of HAB-F ocean-color processing protocols and products as of 2025, updated from 2020. It formalizes current best practices for ingesting, processing, quality-controlling, and disseminating satellite-derived HAB indicators across a diverse and evolving satellite sensor fleet. These guidelines emphasize standardized, reproducible workflows that support both near–real-time operational forecasting and longer-term retrospective analyses.

HAB-F routinely processes data from multiple multispectral and hyperspectral satellite missions operated by the National Aeronautics and Space Administration (NASA), the European Space Agency (ESA), and NOAA, including MODIS, Sentinel-3 OLCI, Sentinel-2 MSI, VIIRS JPSS, and the newly launched PACE OCI, while maintaining continuity with legacy sensors such as SeaWiFS and MERIS (see list of acronyms on page 48 for definitions of sensors). Although these sensors differ in spatial resolution, spectral configuration, and revisit frequency, HAB-F applies harmonized processing approaches to generate consistent Level-3 and Level-4 products across missions.

The standardized product suite described herein focuses on indirect optical proxies for HAB presence and intensity. Core products include chlorophyll-a concentration, the Cyanobacteria Index (CI and CIcyano), Maximum Chlorophyll Index (MCI), Red Band Difference (RBD), diffuse attenuation coefficient (Kd), reflectance-based diagnostic bands, true-color, and enhanced color composites. Collectively, these products support detection of cyanobacteria, dinoflagellates, coccolithophores, and mixed phytoplankton assemblages across optically complex waters. Special emphasis is placed on advanced methods such as CyanNet, a machine-learning framework that enables the construction of a continuous, multi-decadal cyanobacteria bloom record across sensors with differing spectral limitations.

All HAB-F products are generated through the Satellite Automated Processing System (SAPS), a modular Python-based framework that integrates NASA's Ocean Color Science Software (OCSSW) and ESA's Sentinel Application Platform (SNAP). SAPS automates data ingestion, atmospheric correction, reprojection, compositing, product derivation, masking, and metadata generation, ensuring consistent application of quality-control procedures and traceable versioning across products and regions. Products are distributed in standardized GeoTIFF formats with clearly defined scaling, flagging, and metadata conventions.

HAB-F satellite products are disseminated through multiple operational pathways, including the NCCOS HAB Monitoring System (web-based), regional HAB forecast bulletins, seasonal outlooks, and targeted data deliveries to federal, state, tribal, and academic partners. These products directly support NOAA's mission to protect public health, coastal economies, and ecosystem function by providing actionable information to resource managers, decision-makers, and the public.

As new satellite missions, algorithms, and processing capabilities mature, these protocols will continue to be updated. Future efforts will expand sensor integration, refine algorithms for optically complex waters, enhance machine-learning applications, and broaden dissemination to ensure HAB-F products remain scientifically robust, operationally reliable, and responsive to emerging HAB challenges. For questions or more information please contact us at hab@noaa.gov

1. Introduction

The Harmful Algal Bloom Forecasting Branch (HAB-F) at the NOAA National Centers for Coastal Ocean Science (NCCOS) develops and maintains operational and research-grade satellite ocean-color products to support the detection, monitoring, and forecasting of harmful algal blooms (HABs) in U.S. coastal and inland waters. Satellite remote sensing provides wide-area, repeatable observations of ocean color—an optical proxy for phytoplankton biomass, turbidity, dissolved and particulate material, and surface accumulation patterns. These capabilities are foundational to HAB-F forecasting systems, including the NOAA Lake Erie and Gulf Coast HAB Operational Forecast Systems and multiple state and federal bloom-response programs.

This document provides a consolidated and modernized description of the ocean-color processing protocols used by HAB-F as of 2025. It outlines the sensors routinely processed, the reflectance products derived from Level-0 through Level-2 inputs, the algorithms employed to estimate biogeophysical/biogeochemical parameters, and the masking and quality-control procedures applied to produce standardized HAB-F Level-3 and Level-4 products. When relevant, legacy methods are noted for historical continuity, but emphasis is placed on current best practices and harmonized approaches across multispectral and hyperspectral sensors.

The scope of this document is limited to routinely generated and externally disseminated products, which are primarily focused on HAB identification and monitoring. Experimental, pre-publication, or developmental algorithms are excluded to maintain clarity and ensure that all procedures described here are stable, documented, and reproducible. HAB-F routinely updates this protocol as new sensors (e.g., PACE OCI), new machine-learning approaches (e.g., CyanNet), and improved processing pipelines become operational.

2. Satellites and Sensors from which Data are Obtained

HAB-F routinely processes ocean-color data from a range of multispectral and hyperspectral satellite sensors operated by NASA, ESA, and NOAA. These sensors differ in spatial resolution, spectral configuration, revisit frequency, and historical availability, but all provide ocean-color observations suitable for detecting algal biomass, cyanobacterial surface scums, turbidity

patterns, and other optical features relevant to HAB forecasting. Appendix A contains detailed sensor specifications and band characteristics referenced in this section.

Satellite missions incorporated into HAB-F workflows include legacy systems (SeaWiFS, MERIS), active operational sensors (OLCI, VIIRS, MSI, Landsat OLI), MODIS, which is active at the time of this writing but will soon be transitioned to legacy, new hyperspectral observations from PACE OCI, selected commercial small-satellite systems (e.g. Planet SuperDove) under evaluation. Although sensor capabilities vary, the processing framework strives for consistency by applying common atmospheric correction approaches, standardized mapping procedures, and harmonized Level-3 product definitions.

These satellites and sensors are summarized below. Various sensor characteristics can be found in Appendix A, and information on various flagging techniques for each sensor can be found in Appendix B.

2.1 SeaWiFS

The Sea-viewing Wide Field of View Sensor (SeaWiFS) was the first ocean color sensor to deliver routine, near-real time data. SeaWiFS was launched on the SeaStar satellite by Orbital Sciences Corporation in August 1997, and continued operations until 2010. The sensor had a daily revisit time, and a Global Area Coverage swath width of 45 degrees, with a sun synchronous orbit at 705 km. Specifications are found in Appendix 0. HAB-F historically processes SeaWiFS Level-1B and Level-2 data for long-term analyses; the mission remains important for historical context but is no longer active.

2.2 MODIS

The Moderate Resolution Imaging Spectroradiometer (MODIS) is one of the key instruments onboard two NASA polar orbiting satellites, Terra (launched in 1999) and Aqua (launched in 2002). As of 2025, both the Terra and Aqua sensors are still functional and orbit at 705 km but are expected to formally retire in late 2026/early 2027. Terra has a descending node (black line in Figure 1) and has an image acquisition time at ~10:30 AM local time, while Aqua has an ascending node (blue arrow in Figure 1) with an image acquisition time at ~2:30 PM local time. The MODIS sensors have 36 bands, which are detailed in Appendix 0, and a swath width of

2330 km. The primary ocean color bands have a nadir pixel field-of-view of 1.1 km; however, the wide field of view of 110 degrees results in much coarser resolution when further off angle (pixel ground coverage of up to several kilometers). About half of these bands are used for atmospheric or temperature analyses. Each satellite collects data about 5-6 days a week over the continental United States (CONUS). MODIS has operated for over 25 years, far exceeding its intended lifespan, and is expected to cease operations by late 2026/early 2027 (NASA, 2025), similar to SeaWiFS. HAB-F routinely produces imagery from several regions of interest shown in Figure 2.

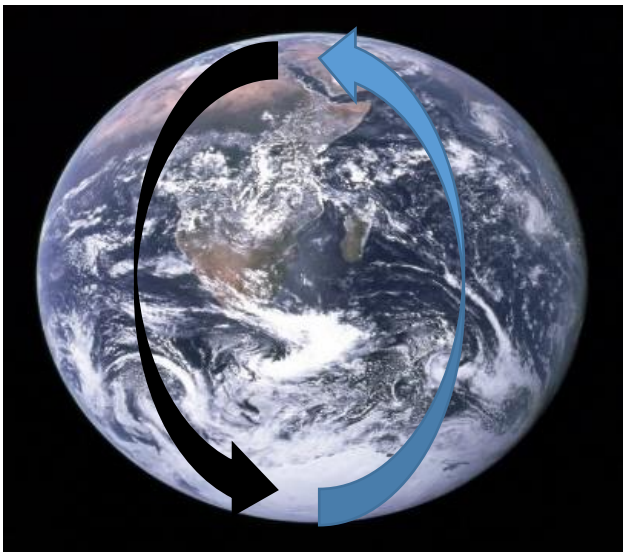

Figure 1. *Orbital difference between Terra (descending node, black arrow) and Aqua (ascending node, blue arrow) orbits.*

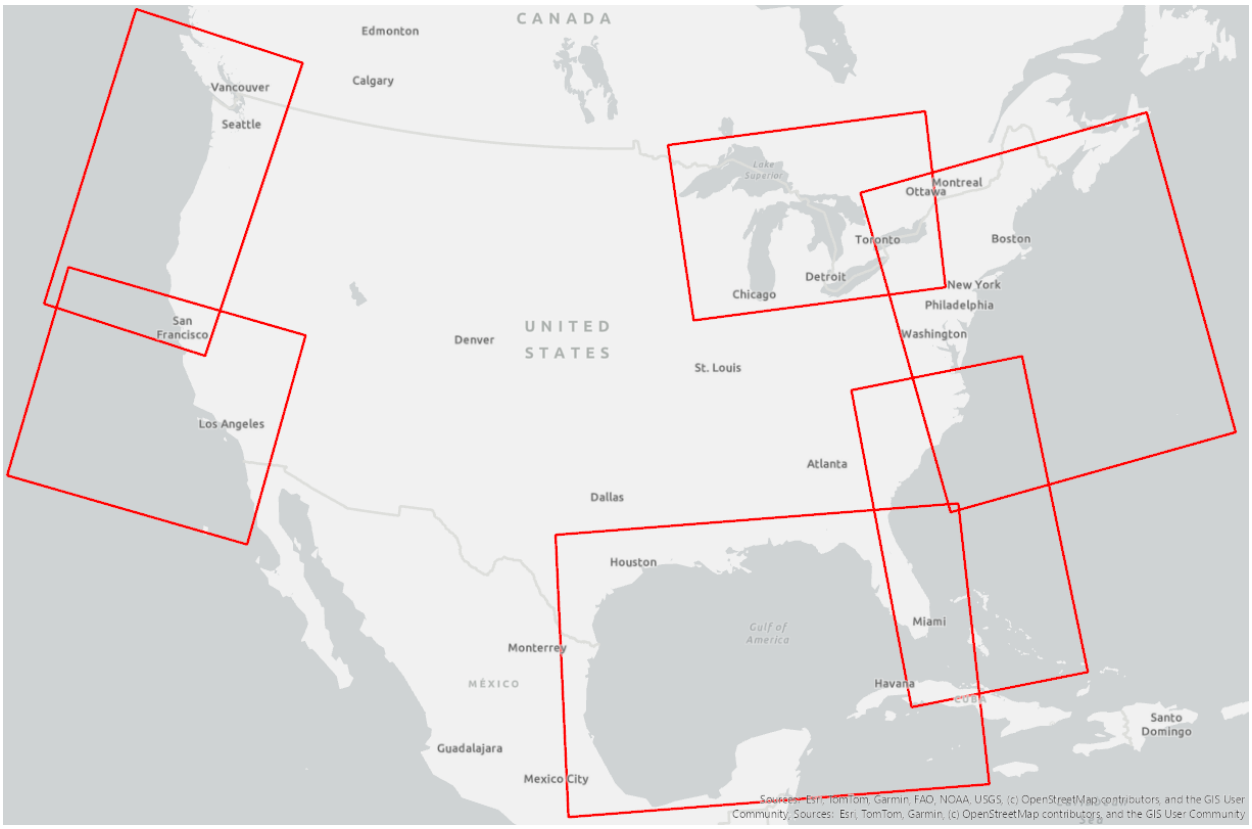

Figure 2. *Geographic regions routinely processed for MODIS by HAB-F.*

2.3 MERIS

Datasets from the Medium Resolution Imaging Spectrometer (MERIS), flown on the Envisat-1 spacecraft, have been used internally at HAB-F since the instrument was launched in April 2002 and continued until the mission ended ten years later in April 2012. MERIS was built and operated by the ESA and provided a swath width of approximately 1150 km in the 68.5-degree field of view. Additional sensor specifications are listed in Appendix A3.

MERIS had a swath width of 1150 km with two spatial-resolution modes: a) Full Resolution (FR) at 300-meter spatial resolution and b) Reduced Resolution (RR) at 1200-meter spatial resolution. RR data were routinely collected globally, with MERIS providing approximately 3-4 days of coverage per week across the continental United States (CONUS). Initially, HAB-F accessed MERIS Level-2 RR files directly from ESA. These were later supplemented with Level-1 FR files obtained from NASA.

Prior to 2008, MERIS FR acquisitions over North America were only partially recorded, resulting in inconsistent spatial/temporal coverage. Depending on the year and region, FR availability ranged from 1 to 3 days per week. Routine direct downlink of MERIS data into Canada began in 2008, which substantially improved FR coverage to approximately 3 days per week, although portions of southern Texas and California experienced slightly reduced coverage.

2.4 OLCI

The Ocean and Land Colour Imager (OLCI), developed and operated by the ESA, is the successor to MERIS and is carried aboard the Sentinel-3 spacecraft series. The first instrument, OLCI on Sentinel-3A, was launched on February 16, 2016, followed by OLCI on Sentinel-3B on April 25, 2018. Subsequent satellites are planned to launch in 2026 (Sentinel 3C) and 2028 (Sentinel 3D). OLCI provides a wider swath than MERIS, approximately 1270 km with the 71° field-of-view, and features improved radiometric resolution. OLCI is pointed 12.6° off nadir away from the sun to reduce the impact of sun glint. The nominal revisit time for one satellite is 3.8 days at the equator and approximately 2.8 days at 30° latitude. With two satellites, the sensor has nearly daily coverage. Nadir spatial resolution is maintained at 300 meters, matching MERIS full-resolution data. Additional sensor specifications are listed in Appendix A4. OLCI regions that HAB-F routinely produces are shown in Figure 3.

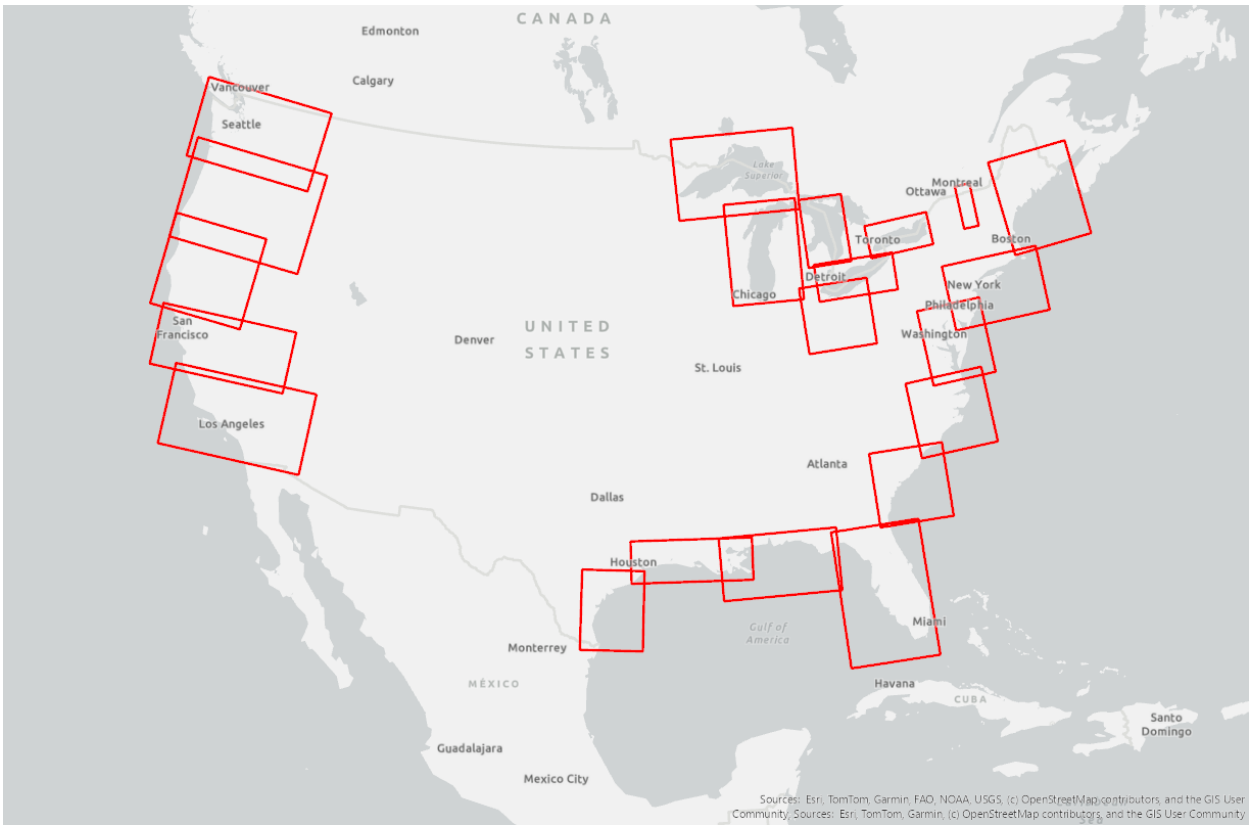

Figure 3. *Geographic regions that are routinely processed by HAB-F for OLCI imagery.*

2.5 MSI

The Multispectral Instrument (MSI) is currently flown on three operational Sentinel-2 spacecraft operated by the ESA. Sentinel-2A was launched on June 23, 2015, followed by Sentinel-2B on March 7, 2017, and Sentinel-2C on September 5, 2024. Sentinel-2C replaced Sentinel-2A as the primary operational platform on January 21, 2025, at which point Sentinel-2A was transitioned to standby status.

All Sentinel-2 satellites are identical in design and provide a 20.6° field of view with a 209-km swath width**,** a combined five-day revisit time**,** and a 10:30 AM local-time descending node. MSI spatial resolution is band-dependent, and the specific resolutions for each band are listed in Appendix A6.

2.6 Landsat

Landsat is the world's longest-running Earth-observing satellite mission, with the first satellite launched in 1972. The Landsat Thematic Mapper (TM) sensor, first launched in 1982 aboard Landsat 4, established the core spectral design that has been carried forward in all subsequent Landsat imaging instruments. The most recent mission, Landsat 9, was launched in September 2021. Both Landsat 8 (launched February 2013) and Landsat 9 remain operational.

Landsat 8 and Landsat 9 each carry two instruments: the Thermal Infrared Sensor (TIRS) and the Operational Land Imager (OLI)**.** OLI, as well as the Landsat 7 ETM+ instrument, includes several visible and near-infrared bands with demonstrated value for inland water applications. In particular, OLI has been effective in delineating cyanobacterial blooms in western Lake Erie (Ho and Michalak, 2017). However, the HAB-F program does not routinely process Landsat imagery despite its high spatial resolution due to its slow revisit rate (e.g. 16 days for Landsat 9). Additional Landsat specifications are listed in Appendix A5.

2.7 VIIRS

The Visible Infrared Imaging Radiometer Suite (VIIRS) is onboard the Suomi National Polar-orbiting Partnership (Suomi NPP) and the NOAA-Joint Polar Satellite System (JPSS), currently NOAA-20 (launched 2017) and NOAA-21 (launched 2022) and are operational, with NOAA-22 planned to be launch in 2027. VIIRS has a swath width of 3060 km and is polar orbiting at 829 km and takes images nearly daily over the CONUS. While VIIRS is not one of the key satellites used within the HAB-F, some data are still processed and distributed in certain areas. VIIRS specifications are provided in Appendix 7.

2.8 PACE

The PACE (Plankton, Aerosol, Cloud, ocean Ecosystem) satellite was launched on February 8, 2024. PACE carries three instruments: the Ocean Color Instrument (OCI) and two multi-angle polarimeters, HARP2 and SPEXone. For the purposes of HAB-F operations and water-quality monitoring, OCI is the primary instrument of interest.

OCI is a hyperspectral ocean color sensor that measures continuously across the 340–895 nm spectral range in 5-nm-wide bands, representing a significant advancement over the multispectral sensors discussed previously. PACE's swath width does not exceed 2500 km, providing near-daily global coverage. The nadir pixel resolution is 1-km, which degrades to much coarser resolutions well away from nadir.

The specific OCI spectral bands available through the SAPS processing system are listed in Appendix 8**.**

2.9 Commercial Small Satellites

Very high resolution, small-satellite constellations are expected to play an increasingly important role in Earth observations in the near future. As of this technical memorandum update, HAB-F does not routinely process imagery from any small-satellite platforms. One of the most promising commercial constellations is Planet's Dove and SuperDove fleet. The Dove constellation comprises approximately 200 CubeSats, each measuring 10 cm × 10 cm × 30 cm and weighing roughly 6 kg, and providing imagery at approximately 3-meter spatial resolution. The original Dove sensors collect data in four spectral bands (blue, green, red, and near-infrared).

The newer SuperDove satellites include eight spectral bands (coastal blue, blue, green I, green, yellow, red, red-edge, and near-infrared) that are similar to ones on the MSI, improving their potential value for coastal and aquatic remote-sensing applications. Although HAB-F does not currently operationalize small-satellite imagery, these systems are being evaluated for their potential to augment cyanobacterial bloom detection, shoreline scum monitoring, and rapid-response assessments when used in conjunction with traditional ocean-color sensors.

3. Products

The HAB-F produces a standardized suite of satellite-derived products used primarily to detect HABs indirectly through optical proxies, most commonly those that estimate chlorophyll-a (Chl-a) concentration. Additional optical parameters, originally developed for unrelated applications,

also provide value for HAB detection, including the diffuse attenuation coefficient (K_d). This section describes the standardized products that are routinely produced and disseminated by the HAB-F.

Satellite data are distributed in several processing "levels," from Level 0 through Level 4, as well as additional derivative products generated from Level 4. Levels 0 through 2 originate from NASA or ESA and are defined as follows:

1. Level 0**:** Raw, unprocessed instrument and payload data. These data are generally unsuitable for scientific analysis without additional calibration processing and are primarily used for instrument diagnostics or calibration activities.
2. Level 1A**:** Reconstructed, unprocessed instrument data that have been time-referenced and annotated with ancillary information. Radiometric and absolute calibration coefficients are included as ancillary metadata, but the radiances remain uncalibrated in terms of geophysical units.
3. Level 1B**:** Level 1A data that have been converted to calibrated sensor units (e.g., radiance) and include basic geometric corrections. These data form the basis for reflectance generation.
4. Level 2A**:** include surface and elevation metrics derived from the geolocated instrument measurements, such as ground elevation, minimum and maximum surface return elevations, energy quantile heights (commonly referred to as *relative height* metrics), and other waveform-derived parameters that characterize the intercepted surface (NASA, 2026).
5. Level 2B**:** re derived from L2A products and represent measurements converted into instrument-specific physical units; not all instruments produce a corresponding L2B product (NASA, 2026)

Levels 3, 4, and all subsequent product layers generated by HAB-F are derived from Levels 0–2 (HAB-F does not keep Level 0-2 products, as those are readily available from NASA or ESA):

- ENVISAT MERIS Level-1B Full Resolution are downloaded from: https://oceancolor.gsfc.nasa.gov/data/10.5067/ENVISAT/MERIS/L1B/FRS/4 [Accessed: 16 December 2025]

- Terra. MODIS Level-0 are downloaded from https://oceandata.sci.gsfc.nasa.gov/directdataaccess/Level-0/Terra-MODIS/ [Accessed: 16 December 2025]
- EUMETSAT OLCI Level 1B Full Resolution - Sentinel-3 are downloaded from https://data.eumetsat.int/product/EO:EUM:DAT:0409 [Accessed: 16 December 2025]

6. Level 3**:** Data mapped to uniform geospatial grids with standardized completeness and consistency. Level 3 files include:
    - Remote sensing reflectance (R_{rs}; sr^{-1})
    - **Rayleigh-corrected surface reflectance (ρ_s; dimensionless)**
      These reflectance fields are corrected for molecular (Rayleigh) scattering and for absorption by atmospheric gases and water vapor. Some standard Level 2 products (e.g., Chl-a) generated by NASA or ESA are also converted to Level 3 grids.
7. Level 4: All products derived from Level 3. These include spatial masks and flagging for land, clouds, and invalid data (invalid meaning inappropriate for the product of interest). HAB-F generates multiple Level 4 product types; the most commonly distributed products are listed in Table 1.

Table 1. *Commonly produced satellite products by the HAB-F.*

Product	**Units**	**Section**
Rayleigh-corrected surface reflectance (ρ_s)	Dimensionless	3
Cyanobacteria Index (CI, CIcyano)	Dimensionless	3.1
Maximum Chlorophyll Index (MCI)	Dimensionless	3.2
Diffuse attenuation coefficient (K_d)	m^{-1}	3.3
Chlorophyll-*a* (*Chl-a*)	mg m^{-3}	3.4
Red band difference (RBD)	Dimensionless	3.5
Rrs(709)	Sr^{-1}	3.6

Scum Index	Dimensionless	3.7
True Color	Dimensionless	3.8
Bloom Color	Dimensionless	3.9

When ρ_s is needed for higher-level products, we generate reflectance using l2gen from NASA's OCSSW software package. For Level-2 ESA products (already containing geophysical parameters such as R_{rs} or Chl-a), HABF will perform only spatial mapping, typically using ESA's Sentinel Application Platform (SNAP). Level 3 files are not distributed due to large file sizes; however, maintaining Level 3 datasets locally enables rapid reprocessing as algorithms evolve, new masks are adopted, or product definitions are updated.

3.1. Cyanobacterial Index (CI)

Cyanobacteria, also known as blue-green algae, represent one of the most pressing environmental challenges affecting coastal and freshwater ecosystems worldwide. The dominant, bloom-forming freshwater cyanobacterium is *Microcystis*, which can produce the hepatotoxin microcystin. This toxin poses significant risks to domestic animals, wildlife, and human health. Effective monitoring of water bodies at risk of cyanobacterial blooms is therefore essential to help mitigate the ecological and public-health impacts associated with both the organism and its toxins.

The Cyanobacteria Index (CI) was first introduced by Wynne et al. (2008) as the Spectral Shape around 681 nm (SS(681)) product, and was later renamed the Cyanobacteria Index by Wynne et al. (2010). The CI was originally developed using MERIS imagery over Lake Erie to detect large, predominantly monospecific cyanobacterial blooms, primarily *Microcystis aeruginosa*. The CI is computed using the following equations. First, the spectral-shape term is calculated as:

$$SS = \rho_{681} - \rho_{665} - (\rho_{709} - \rho_{665}) \times \frac{(681-665)}{(709-665)} \quad (1)$$

where ρ is the top-of-atmosphere reflectance measured at each given wavelength. From this point, the CI is calculated as:

$$CI = SS \times (-1) \quad (2)$$

The complete scaling equations are provided in Appendix D.

False-positive CI values can occur in clear water. To address this, a clear-water test is applied to identify pixels likely to generate false-positive CIs. Any pixel identified as clear water is reclassified as non-detect (see Appendix C).

The CI generally performs well in low- to medium-turbidity waters. However, false positives may also occur in some highly turbid waters. Therefore, a turbidity-screening spectral test is applied to identify pixels where excessive turbidity could generate erroneous CI values; such pixels are likewise classified as non-detect (see Appendix B2).

Clouds are identified using a cloud-specific spectral algorithm. Pixels are classified as invalid if they fail any of several masking tests, including excessive sun glint, proximity to land or vegetation, or algorithm failure.

In addition to the standard product flags (no-data, land, clouds, and saturation; see section 4), an adjacency-effect flag is applied to MERIS and OLCI CI products when false-positive CI values are detected due to any adjacency issue, which is a radiometric contamination problem where the measured signal of a pixel is influenced by light scattered from nearby surfaces and not just the target itself. Land is determined from a GIS-base map of a land/water mask.

Pixels are flagged for adjacency effects when a CI value is present but no corresponding MCI value is detected (see the Maximum Chlorophyll Index Section 3.2 and Appendix B2 for additional detail).

3.1.1. CIcyano

This product is an enhanced version of the standard CI Index. Its development was motivated by the observation that mixed phytoplankton assemblages can yield positive CI values even in the absence of cyanobacteria. This issue was first documented in inland lakes in Ohio but has since been observed in other systems, including Chesapeake Bay, Green Bay and multiple lakes

throughout New England. The phenomenon primarily occurs when eukaryotic algae do not fluoresce, resulting in a spectral shape that can register as CI-positive despite the absence of cyanobacteria.

To address this, a conditional spectral-shape test around 665 nm is used to distinguish pixels dominated by phycocyanin-containing cyanobacteria from those dominated by non-fluorescing eukaryotic algae (Lunetta et al., 2015; Stumpf et al., 2016b). Matthews (2014) applied this same conditional formulation to delineate cyanobacteria blooms.
The spectral-shape term is computed as:

$$SS_{665} = \rho_{665} - \rho_{620} - (\rho_{681} - \rho_{620}) \times \frac{(665 - 620)}{(681 - 620)} \quad (3)$$

The output of Equation (3) determines the classification:

- If SS665 > 0, the pixel is classified as cyanobacteria-dominated, and the resulting product is termed CIcyano.
- If SS665 < 0, the pixel is classified as not cyanobacteria, and the result is termed CInoncyano or CInonfluor.

The CIcyano product is shown graphically in *Figure 4*. The CIcyano value is then computed using:

$$CI = CIcyano + CInoncyano \quad (4)$$

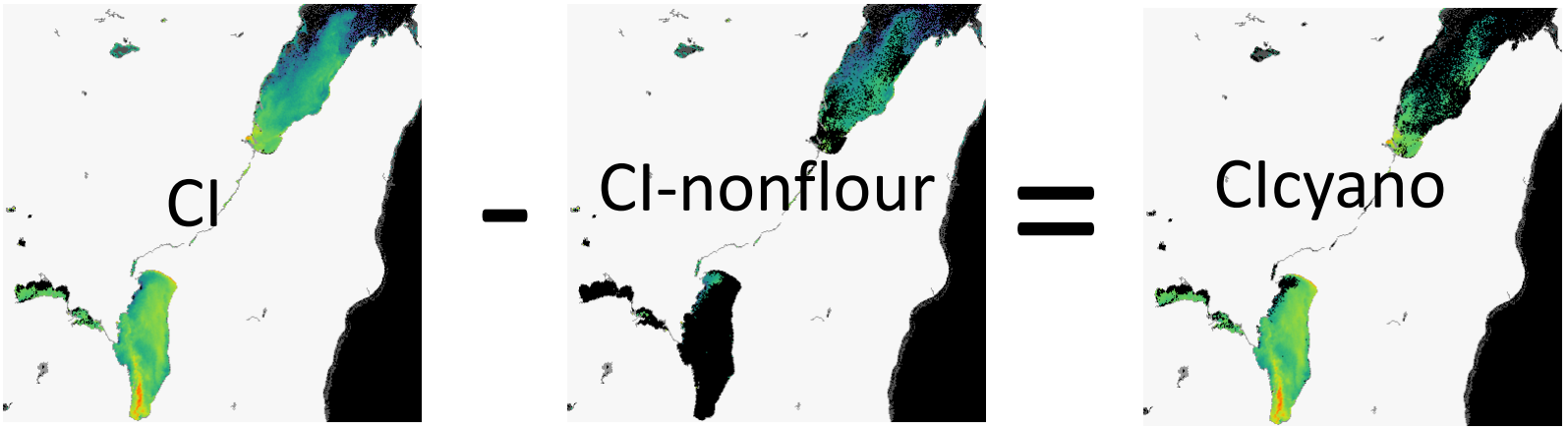

Figure 4. *This example from Green Bay, WI uses OLCI imagery Sept 2, 2025 to illustrate the breakdown of the CI product.*

3.1.2 MODIS Saturation

The CI for Lake Erie historically carried units of per steradian (sr^{-1}), a legacy of the early MERIS Level-2 product formatting and these units were retained in the original MERIS outputs. MODIS CI values were later calibrated to MERIS following Wynne et al. (2013a), and this convention persisted. However, all current Lake Erie CI products are treated as dimensionless**.**

3.1.3 CyanNet

CyanNet was developed to circumvent MODIS saturation issues and to ensure retrieving a CIcyano product from MODIS that is consistent with MERIS and OLCI. CyanNet is a science-informed machine-learning–based satellite product designed to generate a consistent, continuous cyanobacterial bloom record across missions that traditionally cannot be merged, specifically bridging the 2012–2016 observational gap between MERIS and Sentinel-3 OLCI (Mishra et al., 2023). MERIS and OLCI have key cyanobacteria-specific spectral bands (620, 665, 681, 709 nm) required for the Cyanobacteria Index (CIcyano), but MODIS lacks these bands and its red/NIR channels often saturate during intense surface scums. It should be noted that only Terra was used in CyanNet, as its overpass time more closely aligns with that of MERIS and OLCI compared to Aqua. CyanNet overcomes these limitations by training a deep neural network (paired with a logistic regression cyanobacteria classifier) to model MERIS/OLCI-equivalent CIcyano values using MODIS Rayleigh-corrected surface reflectance at 12 MODIS Terra bands. The logistic regression classifier confirms a pixel to be a cyanobacteria pixel, comparable to SS (665)'s purpose in CIcyano (Eq. 3). Whereas the Deep Neural Net quantifies the CIcyano value at the confirmed pixels. The framework also includes a special network,

termed as “CyanNet-S”, for MODIS pixels where red/NIR band saturation prevents a normal CI retrieval (Figure 5).

Briefly, CyanNet-S uses the MODIS bands that are not prone to saturation issues and makes a CIcyano prediction. The result is a MODIS-derived CIcyano product that closely tracks MERIS/OLCI bloom intensity, spatial extent, and seasonal dynamics, enabling the construction of a 25-year continuous cyanobacteria bloom time series (2000–2024). CyanNet performed well not only in the training lake (Lake Okeechobee) but also transferred successfully to various water bodies including Lake Apopka, western Lake Erie, Saginaw Bay, Green Bay, and Lake Winnebago demonstrating strong geographic generalizability. Construction of more than two decades of satellite-based cyanobacteria timeseries, allows long-term trend analysis, bloom phenology studies, and improved monitoring in periods where MERIS/OLCI data do not exist.

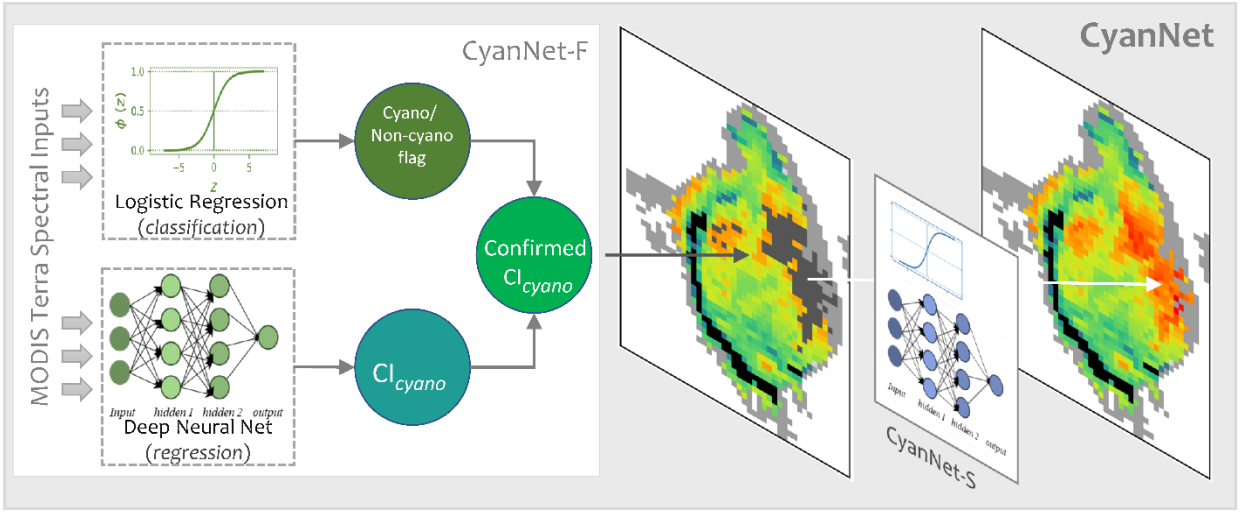

Figure 5. *CyanNet framework highlighting the prediction workflow for saturated and unsaturated pixels in an example Terra-MODIS image in Lake Okeechobee, FL.*

3.2 Maximum Chlorophyll Index (MCI)

The Maximum Chlorophyll Index (MCI) is used to detect high-density patches of Chl-a. It was originally developed by Gower et al. (1999). The MCI formulation begins with the same baseline spectral-shape calculation used as the first step of the CI algorithm, however with the 709 nm

band as the peak. For HAB-F processing, Rayleigh-corrected reflectance (ρ) is used for both OLCI and MERIS sensors.

The spectral-shape term is computed as:

$$MCI = \rho_{709} - \rho_{681} - (\rho_{754} - \rho_{681}) \times \frac{(709 - 681)}{(754 - 681)} \quad (5)$$

ρ_λ is Rayleigh corrected reflectance measured at each given wavelength (nm). Scaling equations associated with MCI generation for converting floats to 8-bit integers are part of tif file metadata as well as provided in Appendix D.

The MCI identifies high Chl-a features regardless of phytoplankton functional group, including cyanobacteria, diatoms, dinoflagellates, and mixed assemblages. A known limitation is that MCI may also return elevated values in waters with high sediment concentrations, which can mimic or obscure algal spectral signatures.

The standard flags applied to the MCI product include no data, land, clouds, and invalid pixels, as detailed in Appendix B2.

3.3 Diffuse Attenuation Coefficient (K_d_*Rhos*)

The diffuse attenuation coefficient (K_d) quantifies the rate at which light diminishes with depth in the water column. K_d is classified as an apparent optical property (AOP), a property that varies with the ambient light field, but it is expressed in the same units (m^{-1}) as an inherent optical property (IOP), which does not depend on the light field. K_d is an indicator of water-column turbidity and is directly influenced by the concentration of light-scattering particles. Please note that the SAPS product is called Kd_Rhos, where the Greek letter ρ is spelled out Rhos.

The K_d product generated by HAB-F is a simplified adaptation of the formulation proposed by Wang et al. (2009; Figure 6).

For the MODIS dataset, K_d is calculated as:

$$K_d = 2.8 \left[\frac{R_\rho(645) - R_\rho(858)}{R_\rho(469) - R_\rho(858)}\right] - 0.69 \quad (6)$$

where Rρ(λ) is the Rayleigh-corrected reflectance at wavelength λ (Tomlinson et al., 2019).

For the MERIS and OLCI sensors, K_d is computed using:

$$K_d = 0.7 \times \left\{ \frac{\left[\frac{(\rho(620)+\rho(665)}{2}\right] - \rho(865)}{\left[\frac{(\rho(442)+\rho(490)}{2}\right] - \rho(865)} \right\} \quad (7)$$

At this point, the respective K_d numbers can be used to calculate a calibrated K_d.

$$K_d calibrated\ (m^{-1}) = (4.0\ \times K_d) - 0.69 \quad (8)$$

The standard masks applied to the K_d product include no data, land, clouds, and invalid pixels, as described in Appendix B.

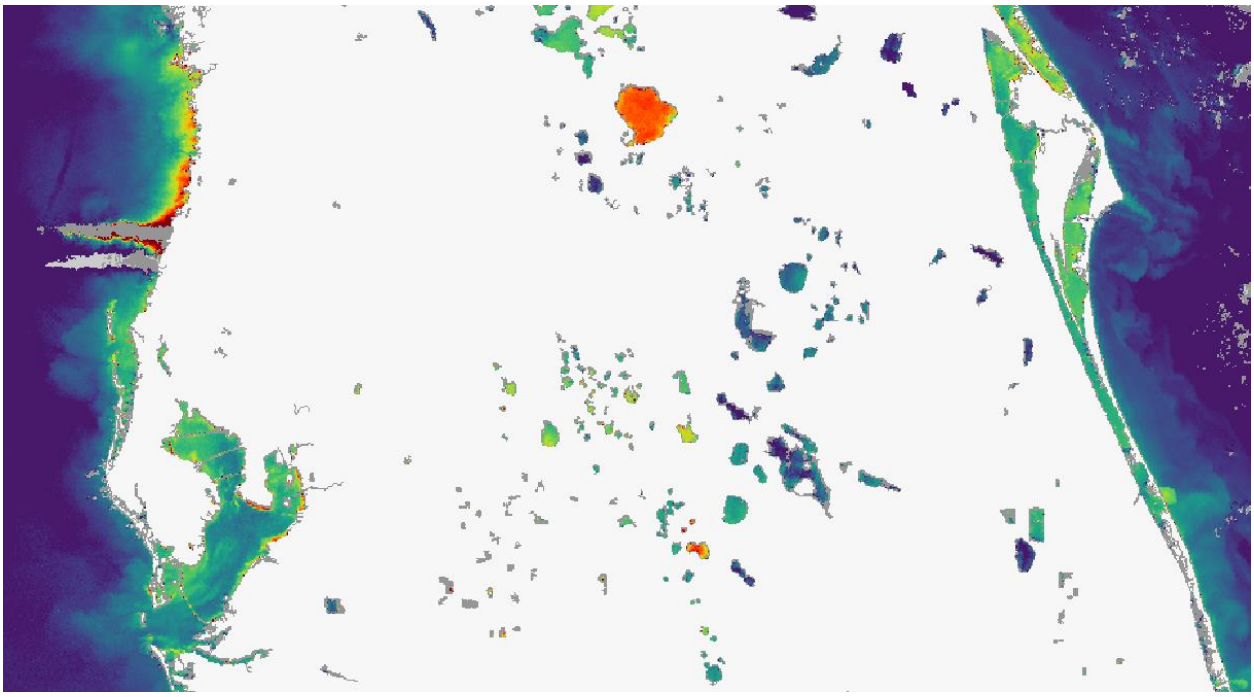

Figure 6. *Shows the Kd product from an OLCI image captured on October 16, 2017 from central Florida. Clearer water are cooler colors, while more turbid water are warmer colors.*

3.4 Chlorophyll-*a*

Chl-a is the primary photosynthetic pigment found across all phytoplankton functional groups. Because it is ubiquitous among cyanobacteria, diatoms, dinoflagellates, and other algae, it is not taxon-specific; however, it serves as a widely used proxy for overall phytoplankton biomass. Satellite-derived Chl-a generally reflects biomass within approximately one optical depth of the water column (i.e., roughly one Secchi depth). Numerous Chl-a retrieval algorithms are

described in the literature. The HAB-F standard processing system uses only a subset of these formulations, and this section highlights those algorithms incorporated into routine operations.

3.4.1 OC4 Chl-a

The OC4 algorithm is the standard NASA global Chl-a algorithm. It was originally developed using SeaWiFS data in the late 1990s (O'Reilly et al., 1999). OC4 is a band-switching algorithm that selects the maximum blue reflectance (depending on the sensor, three or four possible blue bands) and divides it by the green reference band. The blue wavelength with the highest reflectance corresponds to the region of maximum Chl-a absorption, while the green wavelength corresponds to minimum absorption. The band ratio is then inserted into a polynomial equation to retrieve Chl-a concentration.

For OLCI, the OC4 Chl-a algorithm has the form:

$$Chl = 10^{a_0 + a_1 R + a_2 R^2 + a_3 R^3 + a_4 R^4} \quad (9)$$

where the ratio R is:

$$R = log_{10}\left(\frac{max(R_{rs}(\lambda\_blue))}{R_{rs}(560)}\right) \quad (10)$$

For OLCI, the blue bands used in the maximum operator are: 442 nm, 490 nm, and 510 nm. The green reference band is: 560 nm.

Thus, the explicit OLCI form becomes:

$$R = log_{10}\left(\frac{max(R_{rs}(442), R_{rs}(490), R_{rs}(510))}{R_{rs}(560)}\right) \quad (11)$$

The polynomial coefficients a_0, a_1, a_2, a_3, a_4 are those tuned specifically for OLCI's spectral response, known as OC4Me. Accurate Chl-a retrievals using the OC4 algorithm family require a reliable atmospheric correction, as errors in blue-band reflectance strongly impact the band ratio. Standard product flags applied during processing include no data, land, clouds, and invalid pixels. Generally, the OC4 algorithm is most accurate in Case 1 waters, where the optical signature of the water is dominated by phytoplankton and its degradation product. Therefore, the

use of OC4 is most accurate in clear, offshore ocean waters, rather than more optically complex coastal/estuarine or freshwater systems (Figure 8, middle panel).

3.4.2 Chloc4_global

This is the same as the chloc4 product except it is scaled differently to show differences in lower Chl-a water. The two scale bars are shown below. The chloc4_global scale bar extends to 50 mg m^{-3}, where the chloc4 scale bar extends to 135 mg m^{-3}.

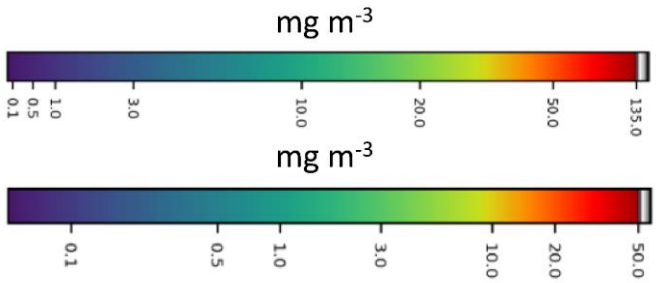

Figure 7. *Shown are the color bars for the 2 chloc4 products. The lower shows the global product designed for more oligotrophic waters, while the top shows the standard product which should be used for more eutrophic waters.*

3.4.3 ESA alg1 and alg2

For the MERIS, ESA has two standard level-2 Chl-*a* products, algal_1 and algal_2 (which have been renamed CHL_OC4ME and CHL_NN in ESA OLCI level 2 files). Algal_1 has the same general form as the OC4 algorithm. Specifically, it is based on the band ratio of the blue to green as provided below.

$$log_{10}(Chl-a) = a_0 + \sum_{i=1}^{4} a_i \left(log_{10} \left[\frac{max\left(R_{rs}(443), R_{rs}(490), R_{rs}(510)\right)}{R_{rs}(560)} \right] \right)^i , \quad (12)$$

where a_0 (0.4502), a_1 (-3.2594), a_2 (3.5227), a_3 (-3.3594), and a_4 (0.9495) are MERIS sensor-specific regression coefficients (ESA, 2012).

This is used for "case-1" waters, where the water's optical properties co-vary with the concentration of phytoplankton biomass and their pigments (similar to the oc4 algorithm mentioned in section 3.4.1. Algal_1 is an iterative equation that eliminates the influence of bi-directionality on the Chl-*a* estimate and as an iterative equation, the final form is not publishable (ESA, 2006). The algal_2 algorithm is based on a neural network prediction and is used for "case-2 waters", where the water optical properties do not co-vary with phytoplankton pigments and are often dominated by inorganic mineral particles and colored dissolved organic matter (CDOM) (Doerffer and Schiller, 2007). The algal_1 and algal_2 algorithms were only produced from the ESA Level 2 files. Standard flags for these algorithms are no data, land, clouds, and invalid pixels.

3.4.4 Chlorophyll RE10

RE10 (Red edge, 2010) describes a Chl-*a* concentration determined by a near-infrared to red ratio as described by Gilerson et al. (2010) with adjustments to coefficients made by Wynne et al. (2022). We implement a modified version of equations 13 and 14 that uses rho_s instead of Rrs.

$$R2 = \frac{(\rho_s(709) - \rho_s(885))}{(\rho_s(665) - \rho_s(885))} \quad (13)$$

$$\text{Chl-}a = (35.75 \times \text{R2} - 14.3)^{1.124} \quad (14)$$

A minimum Chl-a value of 0.4 is assigned when (35.75 × R2 - 14.3) < 0.4. Formerly, this product was referred as Gilerson Chlorophyll. An example RE10 product is shown in Figure 8 (left panel). The algorithm is primarily used in turbid case 2 water such as the Chesapeake Bay (Wynne et al., 2022).

3.4.5 Chlorophyll Switch (chl_switch)

A RE10/OC4 Chl-a switching algorithm was developed to improve estimates in low chlorophyll waters (Chl-a<10 µg L^{-1}) where RE10 has been shown to provide less accurate retrievals than NASA OC4 Chl-a algorithm. (Figure 8, right panel).

$$\text{Chl-}a = \begin{cases} RE10 \text{ Chl-}a, & \text{if RE10} \geq 10 \text{ µg L}^{-1} \\ OC4 \text{ Chl-}a, & \text{if OC4} < 10 \text{ µg L}^{-1} \text{ AND (RE10} < 10 \text{ µg L}^{-1} \text{ OR clear water)} \end{cases} \quad (15)$$

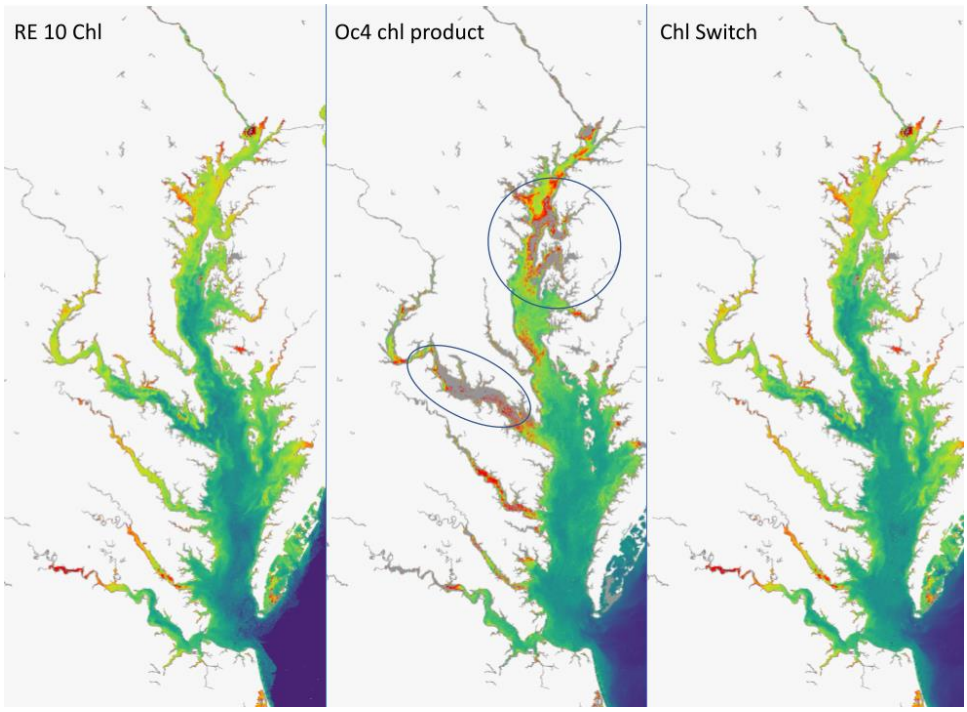

Figure 8. *OLCI imagery from 13 August 2022 showing (left to right) the RE10 product (Section 3.4.4), Oc4 product (Section 3.4.2), and the chlorophyll switch product (Section 3.4.5). The chlorophyll switch product captures the high-chlorophyll features evident in the RE10 product (circled areas) that did not return valid values in OC4, while retaining the more realistic chlorophyll concentrations from OC4 in the bay mouth region. See Figure 7 for color bar.*

3.5 Red Band Difference (RBD)

Red band difference or RBD, also sometimes called Relative Fluorescence, is used as a proxy of relative Chl-a fluorescence and is calculated as the difference between two red spectral bands (Figure 10).

$$RBD = \rho_s(681) - \rho_s(665) \quad (16)$$

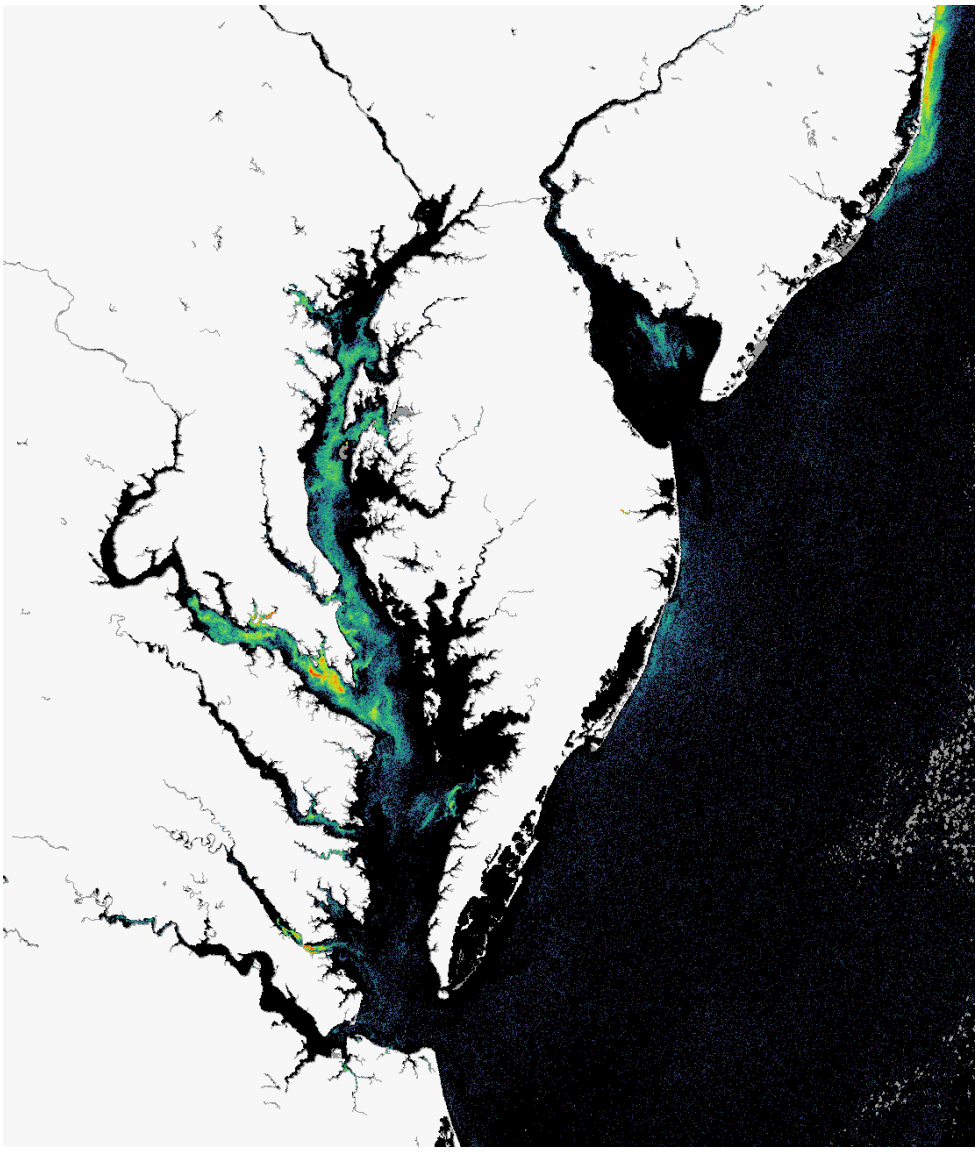

Figure 9. *OLCI Red Band Difference (RBD) image of the Chesapeake Bay from August 13, 2022, the same date as shown in Figure 8. On this date, a bloom of the dinoflagellate, Margalefidinium polykrikoides, was reported in the York River.*

3.6 Rrs709

Remote sensing reflectance at 709 nm (Rrs_{709}) highlights near-infrared backscattering, which becomes strongly elevated in waters containing high phytoplankton biomass, surface-scum cyanobacteria, or suspended sediments, while remaining essentially zero in clear water because pure water absorbs so strongly in the NIR. As a result, Rrs_{709} is a sensitive indicator of dense algal blooms—especially *Microcystis* and other cyanobacteria in the Great Lakes, well as turbid

or resuspended sediment plumes, and it is a key band used in algorithms like the Cyanobacteria Index (CI), and various threshold-based HAB detection tools. In short, high Rrs_{709} generally signals high particulate backscatter from blooms or turbidity, making it an excellent diagnostic band for identifying intense biological or sediment-driven optical events.

3.7 Scum Index (SI)

The scum index (SI) uses the same spectral-shape formulation as the CI and MCI algorithms described in Sections 3.1 and 3.2, but applies a different set of wavelength bands. While the CI uses the 665, 681, and 709 nm bands, the scum index is computed using the 665, 865, and 1012 nm bands. This approach is conceptually similar to the Floating Algal Index (FAI) developed by Hu (2009). The scum index is specifically designed to highlight surface-scum accumulations formed by buoyant cyanobacteria (Figure 10, left panel), and other surface algae such those in the genus *Sargassum*.

$$SI = \rho_{865} - \rho_{665} + (\rho_{665} - \rho_{1012}) \times \frac{(865 - 665)}{(1012 - 665)} \quad (17)$$

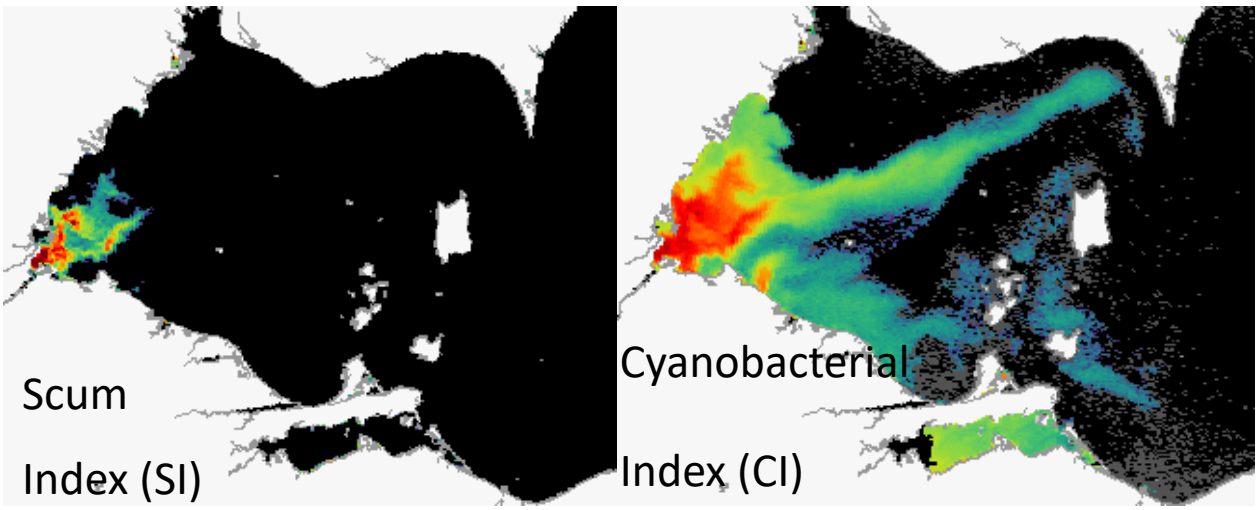

Figure 10. *An example of the Scum Index (SI) product along with the CI product from OLCI imagery captured on Aug 18, 2022. The SI product is designed to show emergent biomass or "scum".*

3.8 True Color

For MERIS and OLCI, the true-color Red Green Blue (RGB) composite is generated using equations 18-20:

- R = ρ(665 nm) (18)
- G = ρ(560 nm) (19)
- B = ρ(490 nm) (20)

For MODIS, the true-color RGB composite is generated using equations 21-23:

- R = ρ(645 nm) (21)
- G = ρ(555 nm) (22)
- B = ρ(469 nm) (23)

where ρ is the top-of-atmosphere reflectance at wavelength the given wavelength.

True-color composite imagery is useful for performing rapid QA/QC of image flagging, as certain features, such as ice, snow, sun glint, sediment plumes, or cloud shadows, are more easily identifiable in RGB than in derived products. True-color images can also be valuable for public communication, where a natural-looking "picture" is more intuitive to interpret (Figure 11). Additionally, because true-color composites retain land features rather than masking them out, they can be advantageous in contexts where shorelines, river plumes, or land-based reference features need to be shown. All true color scenes used the same enhancement, so they are directly comparable for identifying haze, glint, and turbidity.

Figure 11. *True-color OLCI image of the Chesapeake Bay on 13 August 2022. This image corresponds to the same date as the products shown in Figures 8 and 9.*

3.9 Bloom Color

This OLCI product is a three-band composite image similar to the true color product (Section 3.8), Figure 12 (top panel) shows an example of the product along with the corresponding OC4 chlorophyll. It is produced with equations 24-26:

$R = \rho(709) - \rho(885)$ (24)

$G = \rho(560) - \rho(885)$ (25)

$B = \rho(490) - \rho(885)$ (26)

All bloom color products use the same enhancements (how the colors are displayed and scaled), so water features have consistent appearance.

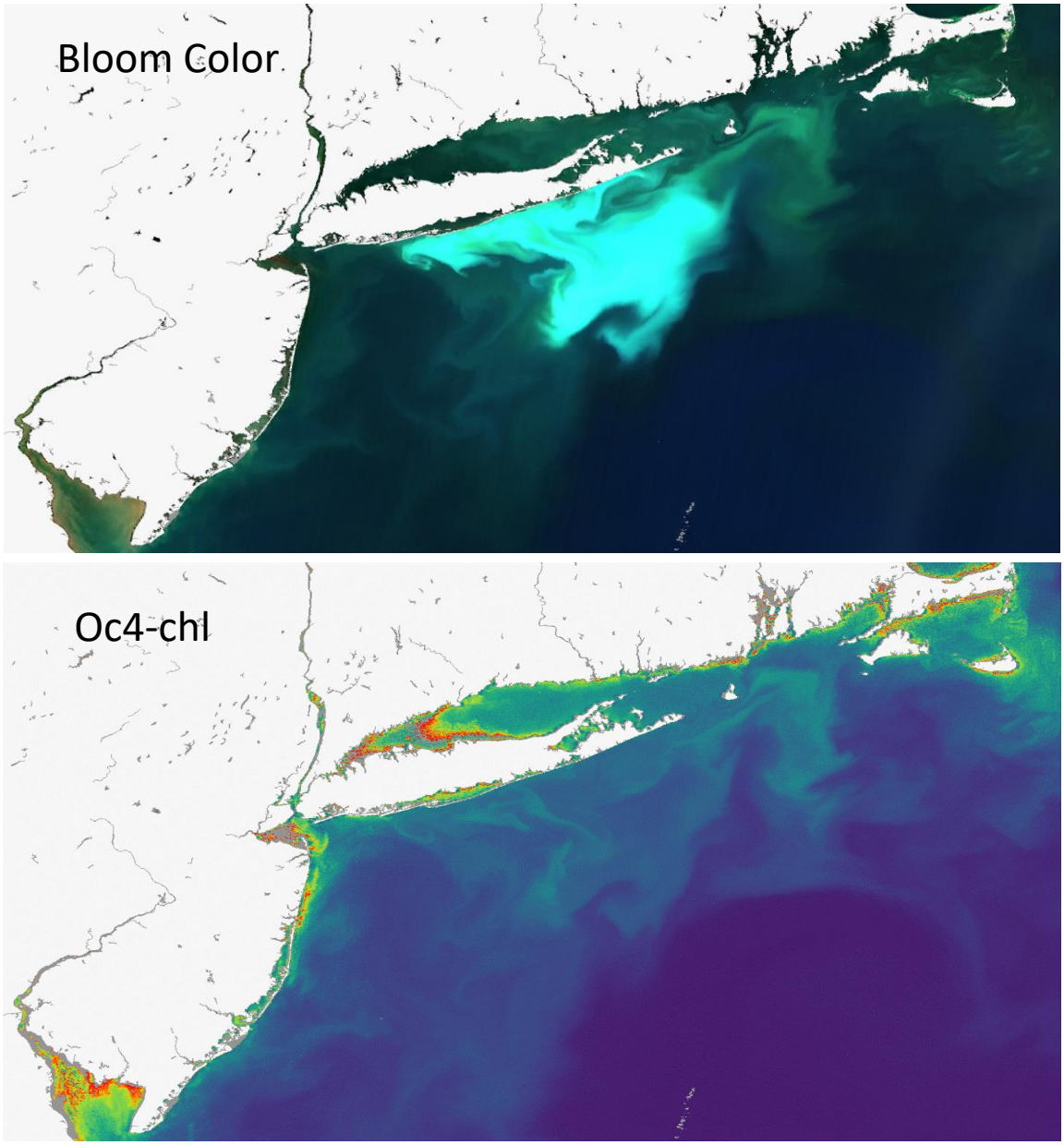

Figure 12. *An example of the Bloom Color OLCI product from the Mid-Atlantic Bight on July 2, 2024. The bright blue feature corresponds to a reported coccolithophore bloom. The bottom image shows the OC4 chlorophyll from the same location and time. This illustrates that different products have the ability to show different blooms. In the example shown here the Bloom Color product helped to locate a calcium carbonate-based bloom.*

4. Satellite Data Processing

SAPS is a collection of custom Python modules (see Appendix E) that automates the downloading and processing of Level-0, Level-1, and Level-2 satellite input files for one or more pre-defined geographic regions. The complete sequence of processing steps is shown in the flowchart in Appendix F. SAPS uses NASA's SeaDAS software package, including the OceanColor Science Software (OCSSW) distributed with SeaDAS, as well as ESA's Sentinel Application Platform (SNAP), specifically, the Sentinel-2 and Sentinel-3 toolboxes, to standardize the conversion of low-level input files into Level-3 GeoTIFFs.

Within SAPS, OCSSW's l2gen program produces Level-2 NetCDF-4 files containing the SAPS-defined product list. These Level-2 files are subsequently mapped and converted into standardized multi-band Level-3 GeoTIFFs using the Reproject operator within SNAP's Graph Processing Tool (GPT). Satellite data are collected in swaths, and each sub-portion of a swath is referred to as a granule. Data from the same day and sensor that overlap a geographic region are composited using a custom Python compositing script. The resulting Level-3 GeoTIFFs are then processed by HAB-F's custom product-generation scripts, which apply sensor-specific algorithms to create single-band GeoTIFFs for each derived product. A dedicated Python script is also used to composite same-day, overlapping Sentinel-3A and Sentinel-3B OLCI scenes.

SAPS executes nightly to process the previous day's available near–real-time data from Sentinel-3A/B OLCI and MODIS Aqua/Terra. Sensor-specific configuration files determine which SAPS-defined geographic regions are processed and which products are generated. When refined ancillary data become available for Aqua or Terra inputs, or when non–time-critical OLCI L1B files are posted, SAPS re-processes the affected datasets and replaces the earlier near-real-time Level-3 files and derived products.

4.1 Product format

The products from the HAB-F have a consistent internal format. Products are distributed as single band GeoTiffs with pixel values ranging between 0-255. The following table describes the standard pixel value meaning (this information is also included within the internal metadata as described later in this section):

Table 2. 8-bit integer data flags in standard products used by the HAB-F.

Value	Description from 2018 on	Description before 2018 reprocessing
0	No detect	No Data
1-249	Valid data (scaled from original value as described in product section)	Valid data
250	Off-scale due to algorithm saturation (may still be considered valid)	Off-scale
251	Adjacency	Not Used
252	Land	Land
253	Cloud/glint	Cloud/glint
254	Invalid or mixed	Not Used
255	No data	Not Used

SAPS specific metadata is created during product creation. It is stored internally within the GeoTiff metadata record. The metadata contains information about product scaling, interpretation of flags and version. SAPS metadata items are prefixed with "SAPS_".
The metadata can be displayed by using a number of commonly available command line utilities including *tiffinfo* and *gdalinfo*. The SAPS script ***run_saps_file_info.py*** may also be used in-house. Sample metadata is listed in Appendix G.

4.2 Product file naming convention

Non-OLCI products have a standard file naming convention as described in Table 3:
<sat>.YYYYJJJ.MMDD.HHmm.L3.<areacode>.<srccode><l2genversion>_<SAPSVersion>_<AlgoscriptVersion>.<productname>.tif
Where:

Table 3: Describes the file naming convention used by HABF for non-OLCI products.

Value	**Description**
<sat>	Name of satellite

Value	Description
YYYY	4-digit year
JJJ	Julian day (zero-prefixed)
MM	Month of year (zero-prefixed)
DD	Day of month (zero-prefixed)
HHmm	Hour & minute (both zero-prefixed) for each granule or swath included in same-day composite
<areacode>	Area code representing the geographic region covered
<srccode>	Level 2 source code (v=SAPS-l2gen,n=NASA,e=ESA,E=SAPS-SNAP)
<l2genversion>	Level 2 generating software version
<SAPSversion>	SAPS software version
<Algoscriptversion>	Version of script generating product
<productname>	Standard product name

As of 2025, OLCI products have a slightly different standard file naming convention by including the satellite ID (“a” or “b”, or “ab” for composites as described in Table 4):

<mission>.YYYYJJJ.MMDD.HHmm.<sat_id>.L3.<areacode>.<srccode><l2genversion>_<SAPS Version>[_<scriptversion>.<productname>].tif

Where:

Table 4: Describes the file naming convention used by HABF for OLCI products.

Value	Description
<mission>	Sentinel-3
YYY	4-digit year

Value	Description
JJJ	Julian day (zero-prefixed)
MM	Month of year (zero-prefixed)
DD	Day of month (zero-prefixed)
HHmm	Hour & minute (both zero-prefixed) for each granule or swath included in same-day composite
<areacode>	Areacode representing the geographic region covered
<srccode>	Level 2 source code (v=SAPS-l2gen,n=NASA,e=ESA,E=SAPS-SNAP)
<sat_id>	Satellite identified (e.g. ‘a’, ‘b’, or ‘ab’ (indicating S3A, S3B, or a composite created from ‘a’ and ‘b’).
<l2genversion>	Level 2 generating software version
<SAPSversion>	SAPS software version
<Algoscriptversion>	Version of script generating product
<productname>	Standard product name

For example: sentinel-3.2017365.1231.1606C.a.L3.LE3.v951T202211_1_3.chloc4.tif would be from the Sentinel-3a spacecraft, on December 31, 2017 at 16:06 GMT. It is a Level-3 (L3) file that is from the OC4 Chl-*a* algorithm.

4.3 Level-3 GeoTiff format

The standard SAPS Level-3 GeoTiff contains a band for each product generated by SAPS. The bands are all 32-bit floating point numbers (i.e., “real”) in the units of the product. The internal TIFFTAG_IMAGEDESCRIPTION contains an ordered “|”-separated list of the band (i.e., product) names. The position of the band name (1-based) indicates the band number within the GeoTiff.

The GPT utility that converts the Level-2 NetCDF file to a GeoTiff, packages the NetCDF metadata into a specialized XML metadata record (tiff tag= 65000) within the GeoTiff. SeaDAS and SNAP read and use this information when loading a Level-3 file. Among other things, this includes product properties such as units and spectral wavelength and parameters used by *l2gen*. The XML metadata can be displayed using the *tiffinfo* utility.

4.4 Flags

Many pixels in satellite imagery are routinely affected by unwanted optical or geometric artifacts. These pixels are considered invalid for one or more of the six primary reasons described in the subsections that follow, and they must be removed to ensure that meaningful scientific analysis can be performed. Because most of the satellite sensors used in HAB-F operations have high temporal resolution but comparatively coarse spatial resolution**,** even a small amount of contamination within a pixel can render the entire pixel invalid.
When this occurs, the affected pixels must be flagged as bad-data values and excluded from subsequent processing steps. The specific flag sets used for each sensor are shown in Appendices B1–B3, corresponding to SeaWiFS, MERIS/OLCI, and MODIS, respectively.

4.4.1 Clouds

Clouds prevent passive remote-sensing instruments, such as all sensors described in this memorandum, which depend on natural sunlight from detecting the water surface, and thus must be removed from analysis. Although limited usable data may occasionally be obtained through thin cirrus for daily imagery, such observations are generally inadequate for constructing climatological datasets.

The custom cloud-flagging procedure described below is applied only when the SAPS Level-3 file used to generate the product was created from Level-1 or Level-0 inputs. These files can be identified by their filenames, in which the L2 source code (srccode) is either “v” or “E” (see the *Product File Naming* section). SAPS Level-3 files with a different srccode rely on the default internal Level-2 cloud flag (L2_flag) for cloud detection and masking.

4.4.2 Glint

Sun glint, or glint, occurs when sunlight is reflected off the surface of the water at or close to the same angle that a satellite views the water. If a pixel is affected by medium to high sun glint the pixel is not usable. This occurs most often near the summer solstice when the sun angle is higher. An example of sun glint is provided in Figure 13.

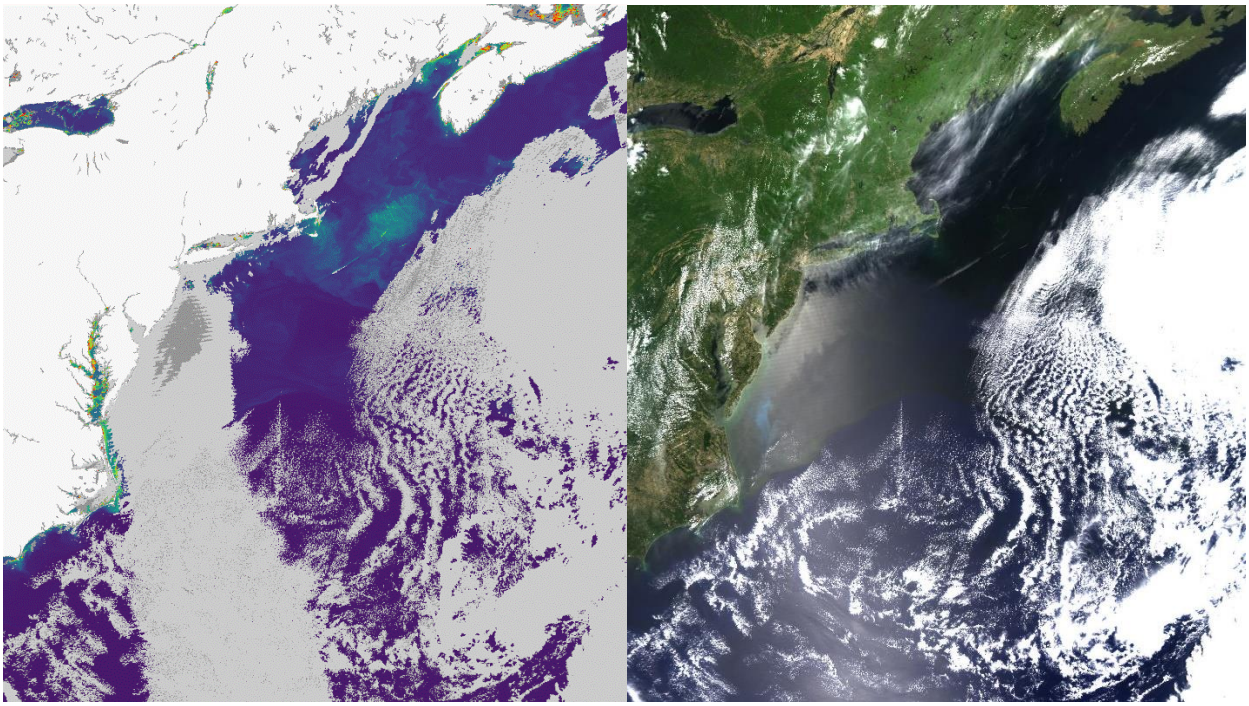

Figure 13. *An example of sun glint, to the left is an Aqua MODIS Chl-a image from June 1, 2014. To the right is the true color image from the same date. Note that the sun glint is masked as clouds.*

4.4.3 Snow and Ice

Snow and ice will present a host of issues and cannot be used in the vast majority of ocean color algorithms. As a result, pixels containing ice must be removed from further analysis. MERIS Differential Snow Index (MDSI) is used for flagging snow and ice.

$$MDSI = \frac{\rho(865) - \rho(885)}{\rho(865) + \rho(885)} \qquad (27)$$

The MDSI can incorrectly flag pixels in dense bloom conditions so with the assumption that snow and ice pixels show little variation in the visible bands, the coefficient of variation calculated in the blue, green and red bands for each pixel is tested against a maximum threshold. A minimum brightness in the NIR band is also required for snow and ice flagging.

This currently used snow and ice algorithm will need improvements. Snow and ice flagging is currently only implemented for MERIS and OLCI products. Ice and snow only occur in certain regions and in certain times of year, however, blooms still may co-occur in these regions and there should be a mechanism to flag ice and snow and be able to create meaningful datasets. This can particularly be advantageous when making composited imagery, such as monthly means.

An example of ice is shown in Figure 14.

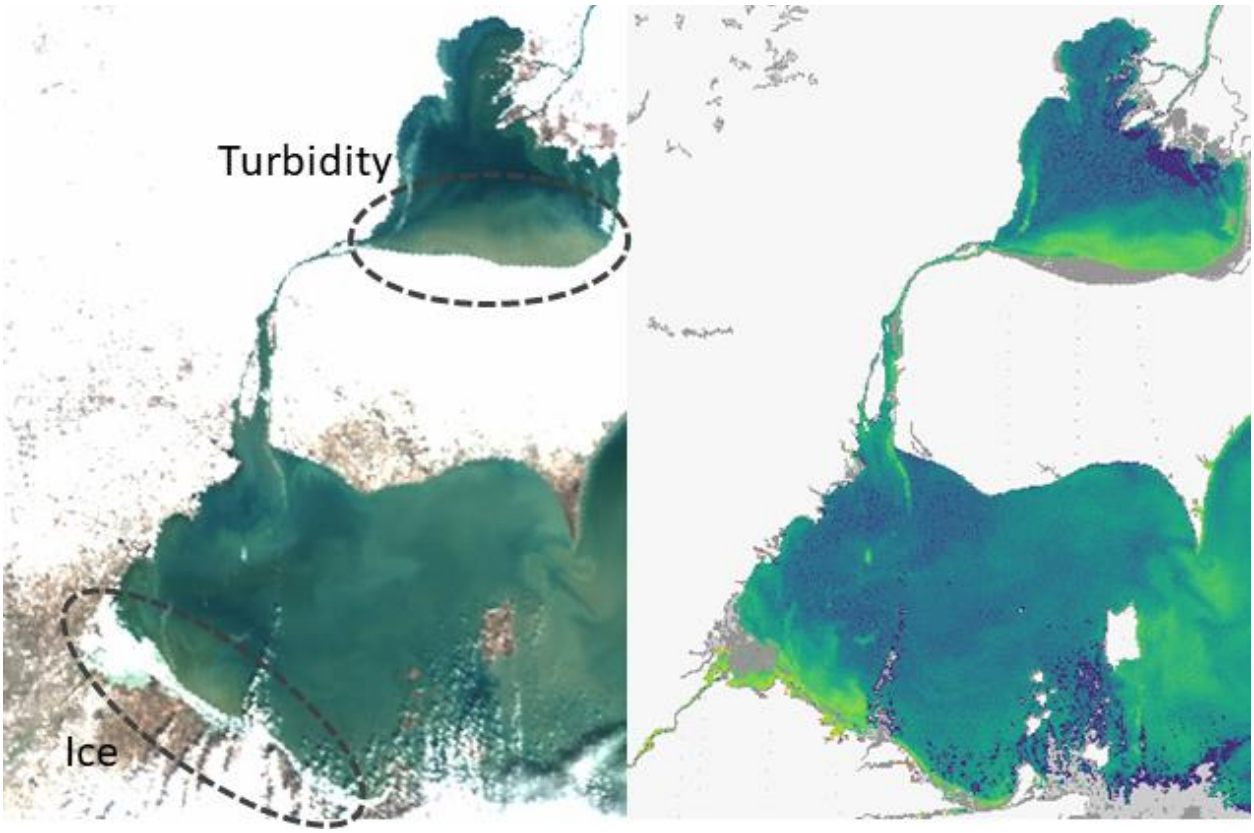

Figure 14. *Left panel: Shows a true color (RGB) composite showing ice cover and turbidity from suspended sediments in western Lake Erie and Lake St. Clair. The right panel shows the derived Chl-a concentration. Both OLCI images are from Jan 27, 2021.*

As can be seen in Figure 14, the limitations are the type of ice. Some thin ice may have reliable retrievals. Some thicker ice may not.

4.4.4 Sensor Saturation

The MODIS' ocean color bands have a more limited dynamic range than all other sensor and bands discussed in this document. As a result, they saturate over bright targets such as intense phytoplankton blooms and suspended sediment plumes. Additionally, clouds and hazy atmospheric conditions can cause saturation.

4.4.5 Algorithm Saturation

Some combination of water turbidity and atmospheric conditions, particularly hazy or slightly glinty conditions, may cause saturation in some algorithms, such as the RBD. An example of algorithmic failure is seen in Figure 15.

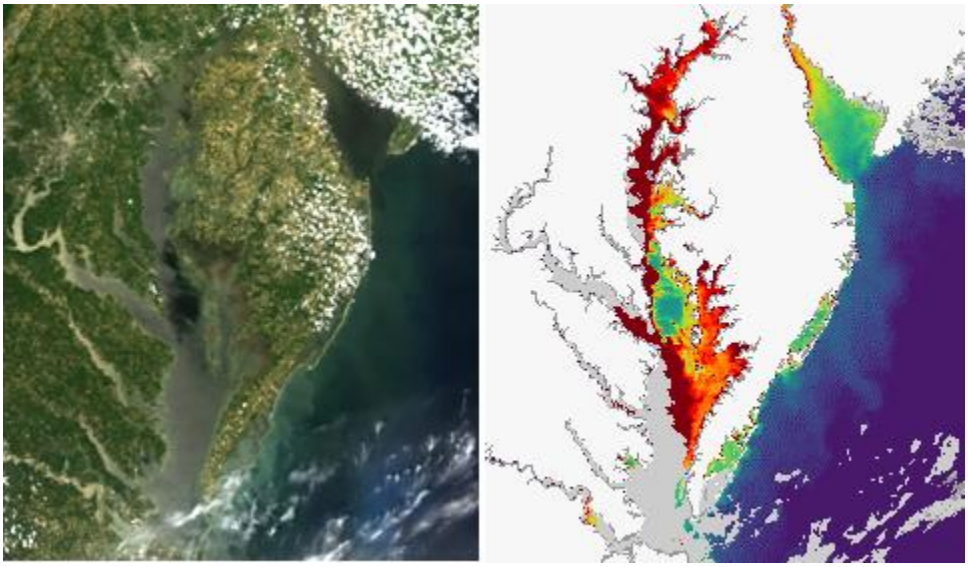

Figure 15. *Left panel: True-color imagery of the Chesapeake Bay acquired by the MODIS-Aqua sensor on 6 June 2014. Right panel: In the corresponding diffuse attenuation coefficient (Kd) product much of the lower portion of the bay is flagged due to sun-glint contamination although other areas of lower glint were not flagged. The dark feature visible in the center of the bay near the mouth of the Potomac River in the left panel corresponds to realistic Kd values whereas regions of dark red are not and due to algorithm failure from glint.*

4.4.6 Land and Dry Lake Bed

We are only concerned with water and not with land in these applications. As a result, all land must be removed. This is obviously most problematic near the coastline. Additionally, if the water is shallow enough (< 1 meter), bottom reflectance is an issue and the pixel must be removed, similar problems can be caused by tides, particularly in areas with large tidal ranges. The following shows the mixed pixel flagging as implemented for MERIS and OLCI (Eq. 19).

$$Mixed_{pixel} = [\rho(885) > \rho(620)]and[\rho(885) > \rho(709)]and[\rho(885) > \rho(754)]and[\rho(885) > 0.01] \quad (19)$$

Additionally, for dry lake beds:

$$Mixed_{pixel} = [\rho(620) > \rho(560)]and[\rho(560) > 0.015]and[\rho(885) > 0.15] \quad (20)$$

Where a mixed pixel is a pixel that has elements of both land and water in it. Additional sensor specific implementations are documented in Appendix B.

5. Compositing

A need for compositing satellite imagery has been demonstrated in previous studies (Stumpf et al., 2012). To support compositing workflows, the HAB-F developed custom code using RSTools, which can be run in ArcGIS Pro (version 3.1.4 or newer)**.** RSTools is available for download from NASA's Ocean Color website: https://oceancolor.gsfc.nasa.gov/about/projects/cyan/.

RSTools can generate annual, seasonal, monthly, and arbitrary time-window composites (e.g., 7-day, 10-day, 14-day). The most commonly used outputs for HAB applications are monthly composites and 10-day composites. The latter are routinely used for cyanobacteria bloom monitoring, where the maximum pixel value within each 10-day period is retained.
This maximum-value approach is widely used because cyanobacteria can mix below the nominal 1-m optical depth and temporarily become undetectable by satellite. These vertical mixing events often last only a few days. As a result, 10-day maximum composites generally provide a cloud-free, representative depiction of bloom conditions, minimizing the risk of underestimating bloom intensity during short-term mixing, cloud cover, or other transient disruptions.

Although RSTools can also produce mean and median composites, the maximum-value composite is typically preferred for bloom detection, particularly in dynamic freshwater systems prone to episodic mixing.

6. Georeferencing

Products are generally released as a georeferenced tagged image file format or (GeoTIFF). Low resolution products (i.e., 1 km) have a custom Albers Equal Area projection with the *latitude of center* and *longitude of center* defined at the tile center. Albers is a conic projection that uses two parallels. Higher resolution products (i.e., <= 300 m) have a Universal Transverse Mercator (UTM) projection.

7. Dissemination and Operational Use

NCCOS has recently begun describing HAB satellite monitoring products and forecasts as an operational service. By that means, disseminating the information produced by the satellite products described here is pivotal for the information to be available and useful for decision-making.

While having a suite of available products is certainly advantageous as a research tool but this should not be the end goal. The National Academy of Sciences (2005) said this: “Much of the federal science and technology investment is intended to help build the base of scientific and technical knowledge and expertise used by government and industry to address important national goals, such as national defense, space exploration, economic growth, and protection of public health and the environment.” In order to do this, data must be effectively distributed to various user groups in a timely and useful manner. In this section, the mechanisms in which products are disseminated are discussed.

7.1 HAB Monitoring System

NCCOS developed the Harmful Algal Bloom Monitoring System (https://coastalscience.noaa.gov/science-areas/habs/hab-monitoring-system/) to routinely deliver near real-time products for use in locating, monitoring and quantifying algal blooms in the

coastal and Great Lake regions of the US. This application delivers a suite of bloom detection products in the form of geographic based images. At this time, products are available for selected regions including Lake Erie, Chesapeake Bay, Green Bay, Saginaw Bay, Lake Pontchartrain, Albemarle Sound, Southwest Florida, Lake Champlain, and Lake Okeechobee. New products are being evaluated, and new regions are being considered; as they are proven useful, they will be made available through this system. A new national level map is currently being developed with the goal of having HAB monitoring system available for coastal and Great Lakes region of CONUS in the near future.

7.2 HAB Forecasts

Regionally-specific HAB bulletins have been an effective means for communicating and disseminating short term HAB forecasts (< 1 week) at various locations. Regional forecasts are available on the NCCOS HAB Forecasting page at https://coastalscience.noaa.gov/science-areas/habs/hab-forecasts/. Depending on the region and season, forecast products are typically updated from hourly to daily.

Historically, forecast models and products were developed within NCCOS or by external partners, experimentally produced and tested within NCCOS and then transferred to run operationally at NOAA's Center for Operational Oceanographic Products and Services (CO-OPS). As of 2021, the responsibility for running and producing the operational forecasts was transferred to the NCCOS HAB-F. Examples of operational forecasts developed within the NCCOS HAB-F are *Karenia brevis* (red tide) blooms in the west Florida Shelf (Stumpf et al., 2003); *Karenia brevis* blooms along the Texas coast (Wynne et al., 2005), and Cyanobacteria blooms in western Lake Erie (Wynne et al., 2013). *Alexandrium catenella* blooms are also being operationally forecasted in the Gulf of Maine (Li et al., 2009; Li et al., 2020), although these forecasts typically do not rely on ocean color imagery. See Table 5 for a list of forecasts.

Additionally, the HAB-F has produced seasonal forecasts on cyanobacteria blooms in Lake Erie since 2012 (Stumpf et al., 2012; Stumpf et al., 2016). These forecasts are disseminated as weekly bulletins and kicked off by a NOAA press release, typically in early July. They are also delivered at a press event at the Ohio State University Stone Laboratory. An example of a press

release can be found at https://nccospublicstor.blob.core.windows.net/hab-data/bulletins/lake-erie/current/bulletin_current.pdf.

Table 5: Shows the regions where forecasts are made by HABF

Forecast	Forecast Region
1	Lake Erie
2	Gulf Coast (FL and TX)
3	Gulf of Maine
4	Chesapeake Bay (developmental)
5	Other event response capabilities

7.3 Other

Products can be disseminated in other outlets on demand as needed. For example, we have been contacted by the USGS to provide them estimates of cyanobacterial concentration for a bioenergetics model to approximate if there are adequate food source to sustain a population of invasive bigheaded carps. These data were delivered onto the USGS ftp server.
There is an NCCOS $K_d(490)$ product distributed by Coastwatch here:
https://eastcoast.coastwatch.noaa.gov/cw_k490_hires.php

There is a HAB Data Explorer page put out by NCCOS (NCCOS, 2025) that has select image products available for the MODIS, MSI, and OLCI sensors. In conjunction with a larger NCCOS-wide effort, HAB-F is currently exploring migrating processing and all data and products to the cloud hosted by Azure.

8. Future work

We will add additional sensors and satellite missions. Further dissemination of developed products would also be used and described herein. HAB-F continuously explores new satellite capabilities to improve the spatial and temporal resolution of products. We have begun exploring PACE's hyperspectral capabilities to increase available data, act as a band integrator between satellite sensors, and to explore novel research such as species and functional type separability.

Smallsats offer us the potential ability to acquire more temporal data at 3 m resolution which could expand spatial coverage to smaller water bodies, such as reservoirs, where HABs can cause particularly acute problems.

References

Amin, R., Zhou, J., Gilerson, A., Gross, B., Moshary, F., & Ahmed, S. (2009). Novel optical techniques for detecting and classifying toxic *Karenia brevis* blooms using satellite imagery. *Optics Express*, 17, 9126–9144.

Baith, K., Lindsay, R., & McClain, C. R. (2001). SeaDAS: A data analysis system for ocean color satellite sensors. *Eos, Transactions American Geophysical Union*, 82, 202.

Doerffer, R., & Schiller, H. (2007). The MERIS Case 2 water algorithm. *International Journal of Remote Sensing*, 28, 517–535.

ESA. (2006). *MERIS Product Handbook*. Retrieved June 20, 2018, from https://earth.esa.int/pub/ESA_DOC/ENVISAT/MERIS/meris.ProductHandbook.2_1.pdf

ESA. (2012). *MERIS 3rd Data Reprocessing Validation Report*. Retrieved June 21, 2018, from https://earth.esa.int/documents/700255/707222/A879-NT-017-ACR_v1.0.pdf/6fa86bec-9945-4e39-808e-3801f2e3962b

Gilerson, A., Gitelson, A., Zhou, J., Gurlin, D., Moses, W., Ioannou, I., & Ahmed, S. (2010). Algorithms for remote estimation of chlorophyll-a in coastal and inland waters using red and near-infrared bands. *Optics Express*, 18, 24109–24125.

Gower, J. F. R., Doerffer, R., & Borstad, G. A. (1999). Interpretation of the 685 nm peak in water-leaving radiance spectra: fluorescence, absorption, scattering, and MERIS observations. *International Journal of Remote Sensing*, 20, 1771–1786.

Ho, J. C., & Michalak, A. M. (2017). Phytoplankton blooms in Lake Erie impacted by both long-term and springtime phosphorus loading. *Journal of Great Lakes Research*, 43, 221–228.

Hu, C. (2009). A novel ocean color index to detect floating algae in the global oceans. *Remote Sensing of Environment*, 113(10), 2118–2129.

Li, Y., He, R., McGillicuddy, D. J. Jr., Anderson, D. M., & Keafer, B. A. (2009). Investigation of the 2006 *Alexandrium fundyense* bloom in the Gulf of Maine: in situ observations and numerical modeling. *Continental Shelf Research*, 29(17), 2069–2082.

Li, Y., Stumpf, R. P., McGillicuddy, D. J. Jr., & He, R. (2020). Dynamics of an intense *Alexandrium catenella* red tide in the Gulf of Maine: satellite observations and numerical modeling. *Harmful Algae*, 99, 101927.

Lunetta, R. S., Schaeffer, B. A., Stumpf, R. P., Keith, D. L., Jacobs, S. A., & Murphy, M. S. (2015). Evaluation of cyanobacteria cell-count detection derived from MERIS imagery across the eastern USA. *Remote Sensing of Environment*, 157, 24–34.

Matthews, M. W. (2014). Eutrophication and cyanobacterial blooms in South African inland waters: 10 years of MERIS observations. *Remote Sensing of Environment*, 155, 161–177.

Mishra, S., Stumpf, R. P., & Meredith, A. (2023). Constructing a consistent and continuous cyanobacteria bloom monitoring product from multi-mission ocean color instruments. *Remote Sensing*, 15(22), 5291.

Mishra, S., Stumpf, R. P., Wynne, T. T., & Hounshell, A. (Accepted). Two decades of cyanobacterial bloom dynamics in the Great Lakes: Insights from multi-mission ocean color sensors. *Environmental Research: Ecology*.

NASA. 2025. https://ladsweb.modaps.eosdis.nasa.gov/learn/modis-to-viirs-transition/#:~:text=Further%2C%20due%20to%20fuel%20limitations,mean%20local%20times%20(MLT) Accessed online Dec. 12, 2025.

NASA. 2026. https://www.earthdata.nasa.gov/learn/earth-observation-data-basics/data-processing-levels. Accessed online Jan 2, 2026.

National Academy of Sciences (US). (1995). *Allocating Federal Funds for Science and Technology*. Supplement 1: Evolution and Impact of Federal Government Support for R&D. Washington, DC: National Academies Press. Retrieved from https://www.ncbi.nlm.nih.gov/books/NBK45556/

NCCOS. (2025). HAB Data Explorer. Accessed September 24, 2025, from https://app.coastalscience.noaa.gov/habs_explorer/index.php?path=NFk5UGZnNlRBYTdrMmFNOEFtSTh3QT09&uri=VWtuM1UzbVNVN0RsZzJMeTJvNlNpM29OalF0WTFQQjVZVnpuS3o5bnh1Ym0vYWhtWEh4ck1hREVUamE4SDZ0M0JnSnNMaHk4U2YyaTc0R04zM2ZId09ud2FVUlZlL1hhdm5jandUS0x6R289&type=bllEUXA3TmhSK21RVDlqbFYxMmEwdz09

NOAA. (2017). Lake Erie Harmful Algal Bloom Bulletin. Accessed January 9, 2018, from https://coastalscience.noaa.gov/exit/?url=https%3A%2F%2Fnccospublicstor.blob.core.windows.net%2Fhab-data%2Fbulletins%2Flake-erie%2Fcurrent%2Fbulletin_current.pdf

O'Reilly, J. E., Maritorena, S., Mitchell, B. G., Siegel, D. A., Carder, K. L., Garver, S. A., Kahru, M., & McClain, C. R. (1998). Ocean color chlorophyll algorithms for SeaWiFS. *Journal of Geophysical Research*, 103, 24937–24953.

Stumpf, R. P., & Pennock, J. R. (1989). Calibration of a general optical equation for remote sensing of suspended sediments in a moderately turbid estuary. *Journal of Geophysical Research*, 94, 14363–14371.

Stumpf, R. P., Culver, M. E., Tester, P. A., Tomlinson, M., Kirkpatrick, G. J., Pederson, B. A., Truby, E., Ransibrahmanakul, V., & Soracco, M. (2003). Monitoring *Karenia brevis* blooms in the Gulf of Mexico using satellite ocean color imagery and other data. *Harmful Algae*, 2, 147–160.

Stumpf, R. P., Johnson, L. T., Wynne, T. T., & Baker, D. B. (2016a). Forecasting annual cyanobacterial bloom biomass to inform management decisions in Lake Erie. *Journal of Great Lakes Research*, 42, 1174–1183.

Stumpf, R.P., Davis, T.W., Wynne, T.T., Graham, J.L., Loftin, K.A., Johengen, T.H., Gossiaux, D., Palladino, D. and Burtner, A., 2016b. Challenges for mapping cyanotoxin patterns from remote sensing of cyanobacteria. Harmful algae, 54, pp.160-173.

Stumpf, R. P., Wynne, T. T., Baker, D. B., & Fahnenstiel, G. L. (2012). Interannual variability of cyanobacterial blooms in Lake Erie. *PLoS ONE*, 7(8), e42444. https://doi.org/10.1371/journal.pone.0042444

Tomlinson, M. C., Stumpf, R. P., & Vogel, R. L. (2019). Approximation of diffuse attenuation (Kd) for MODIS high-resolution bands. *Remote Sensing Letters*, 10, 178–185.

Wang, M., & Shi, W. (2007). The NIR–SWIR combined atmospheric correction approach for MODIS ocean color data processing. *Optics Express*, 15(24), 15722.

Wang, M., Son, S. H., & Harding, L. W. (2009). Retrieval of diffuse attenuation coefficient in Chesapeake Bay and turbid ocean regions for satellite ocean color applications. *Journal of Geophysical Research: Oceans*, 114(C10).

Wynne, T. T., Stumpf, R. P., Tomlinson, M. C., Ransibrahmanakul, V., & Villareal, T. A. (2005). Detecting *Karenia brevis* blooms and algal resuspension in the western Gulf of Mexico with satellite ocean color imagery. *Harmful Algae*, 4(6), 992–1003.

Wynne, T. T., Stumpf, R. P., Tomlinson, M. C., Warner, R. A., Tester, P. A., Dyble, J., & Fahnenstiel, G. L. (2008). Relating spectral shape to cyanobacterial blooms in the Laurentian Great Lakes. *International Journal of Remote Sensing*, 29, 3665–3672.

Wynne, T. T., Stumpf, R. P., Tomlinson, M. C., & Dyble, J. (2010). Characterizing a cyanobacterial bloom in western Lake Erie using satellite imagery and meteorological data. *Limnology and Oceanography*, 55, 2025–2036.

Wynne, T. T., Stumpf, R. P., & Briggs, T. O. (2013a). Comparing MODIS and MERIS spectral shapes for cyanobacterial bloom detection. *International Journal of Remote Sensing*.

Wynne, T. T., Stumpf, R. P., Tomlinson, M. C., Fahnenstiel, G. L., Schwab, D. J., Dyble, J., & Joshi, S. (2013). Evolution of a cyanobacterial bloom forecast system in western Lake Erie: Development and initial evaluation. *Journal of Great Lakes Research*, 39, 90–99.

Wynne, T. T., Tomlinson, M. C., Briggs, T. O., Mishra, S., Meredith, A., Vogel, R. L., & Stumpf, R. P. (2022). Evaluating the efficacy of five chlorophyll-a algorithms in Chesapeake Bay (USA) for operational monitoring and assessment. *Journal of Marine Science and Engineering*, 10(8), 1104. https://doi.org/10.3390/jmse10081104

Acronyms

Acronym	Description
AOP	Apparent Optical Property; optical property dependent on the ambient light field.
CI	Cyanobacteria Index.
CInoncyano	Conditional spectral-shape indicator for non-cyanobacteria blooms (negative CI condition).
CInonflour	Conditional spectral-shape indicator for non-fluorescing phytoplankton.
CONUS	Continental United States
ESA	European Space Agency.
FAI	Floating Algal Index used to detect floating algae (Hu, 2009).
FR	Full-Resolution MERIS imagery (300 m pixel size).
HAB	Harmful Algal Bloom.
HAB-F	Harmful Algal Bloom Forecasting Branch (within NCCOS).
HARP2	Hyper-Angular Rainbow Polarimeter 2; a multi-angle polarimeter on NASA's PACE mission.
IOP	Inherent Optical Property; optical property independent of the ambient light field.
K_d	Diffuse attenuation coefficient.
l2gen	NASA OCSSW program generating Level-2 geophysical products from Level-1 radiances.
MDSI	MERIS Differential Snow Index; a spectral index used for flagging snow and ice in MERIS and OLCI data.
MCI	Maximum Chlorophyll Index.
MERIS	Medium Resolution Imaging Spectrometer.
MODIS	Moderate Resolution Imaging Spectroradiometer.
MSI	Multispectral Instrument (Sentinel-2).
NASA	National Aeronautics and Space Administration.
NDCI	Normalized Difference Chlorophyll Index.
NCCOS	National Centers for Coastal Ocean Science.
NetCDF	Network Common Data Format.
NIR	Near Infrared.
NOAA	National Oceanic and Atmospheric Administration.
OCI	Ocean Color Instrument (NASA PACE mission).
OLI	Operational Land Imager on Landsat.
OLCI	Ocean and Land Colour Imager (Sentinel-3).
OCSSW	Ocean Color Science Software (SeaDAS processing system).
PACE	Plankton, Aerosol, Cloud, ocean Ecosystem (NASA mission).
RGB	Red–Green–Blue color composite.
RR	Reduced-Resolution MERIS imagery (1200 m pixel size).
R_{rs}	Remote Sensing Reflectance (sr^{-1}).

ρ_s	Rayleigh-corrected surface reflectance (dimensionless).
SAPS	Satellite Automated Processing System (HAB-F processing framework).
SeaDAS	SeaWiFS Data Analysis System.
SeaWiFS	Sea-viewing Wide Field-of-view Sensor.
SNAP	Sentinel Application Platform (ESA).
SPEXone	Spectro-Polarimeter for Exploration; a high-accuracy polarization spectrometer on NASA's PACE mission.
SWIR	ShortWave InfraRed.
TIRS	Thermal Infrared Sensor on Landsat.
UTM	Universal Transverse Mercator projection.
VIIRS	Visible Infrared Imaging Radiometer SuitA1:B43e.

Appendices

Appendix A: Sensor Characteristics

A1. SeaWiFS band characteristics from Section 2.1

Band	Band width	Spatial Resolution	Application
1	402-422	1100 meters	Yellow Substance
2	433-453	1100 meters	Chl absorption max
3	480-500	1100 meters	Chl and other pigments
4	500-520	1100 meters	Sediment and red tides
5	545-565	1100 meters	Chl absorption minimum
6	660-680	1100 meters	Chl absorption
7	745-785	1100 meters	Ocean color /phytoplankton/biogeochemistry
8	845-885	1100 meters	Ocean color /phytoplankton/biogeochemistry

A2. MODIS band characteristics from Section 2.2

Band	Bandwidth (nm)	Spectral radiance	Spatial Resolution	Primary Use
1	620-670	21.8	250 meters	Land/cloud aerosol boundary
2	841-876	24.7	250 meters	Land/cloud aerosol boundary
3	459-479	35.3	500 meters	Land/cloud aerosol properties
4	545-565	29.0	500 meters	Land/cloud aerosol properties
5	1230-1250	5.4	500 meters	Land/cloud aerosol properties
6	1628-1652	7.3	500 meters	Land/cloud aerosol properties
7	2105-2155	1.0	500 meters	Land/cloud aerosol properties
8	405-420	44.9	1000 meters	Ocean color /phytoplankton/biogeochemistry
9	438-493	41.9	1000 meters	Ocean color /phytoplankton/biogeochemistry
10	483-493	32.1	1000 meters	Ocean color /phytoplankton/biogeochemistry

11	526-536	27.9	1000 meters	Ocean color /phytoplankton/biogeochemistry
12	546-556	21.0	1000 meters	Ocean color /phytoplankton/biogeochemistry
13	662-672	9.5	1000 meters	Ocean color /phytoplankton/biogeochemistry
14	673-683	8.7	1000 meters	Ocean color /phytoplankton/biogeochemistry
15	743-753	10.2	1000 meters	Ocean color /phytoplankton/biogeochemistry
16	862-877	6.2	1000 meters	Ocean color /phytoplankton/biogeochemistry
17	890-920	10.0	1000 meters	Atmospheric water vapor
18	931-941	3.6	1000 meters	Atmospheric water vapor
19	915-965	15.0	1000 meters	Atmospheric water vapor
20	3660-3840	0.45	1000 meters	Surface/cloud temperature
21	3929-3989	2.38	1000 meters	Surface/cloud temperature
22	3929-3989	0.67	1000 meters	Surface/cloud temperature
23	4020-4080	0.79	1000 meters	Surface/cloud temperature
24	4433-4498	0.17	1000 meters	Atmospheric Temperature
25	4482-4549	0.59	1000 meters	Atmospheric Temperature
26	1360-1390	6.0	1000 meters	Cloud water vapor
27	6535-6895	1.16	1000 meters	Cloud water vapor
28	7175-7475	2.18	1000 meters	Cloud water vapor
29	8400-8700	9.58	1000 meters	Cloud properties
30	9580-9880	3.69	1000 meters	Ozone
31	10780-11280	9.55	1000 meters	Surface cloud temperature
32	11770-12270	8.94	1000 meters	Surface cloud temperature
33	13185-13485	4.52	1000 meters	Cloud top altitude
34	13485-13785	3.76	1000 meters	Cloud top altitude
35	13785-14085	3.11	1000 meters	Cloud top altitude
36	14085-14385	2.08	1000 meters	Cloud top altitude

A3. MERIS band characteristics from Section 2.3

Band Number	Band Center (nm)	Band Width (nm)	Application
1	412.5	10	Yellow substance
2	442.5	10	Chl-*a* absorption maximum
3	490	10	Chl-*a* and other pigments
4	510	10	Sediment and red tides
5	560	10	Chl-*a* absorption minimum
6	620	10	Suspended sediment
7	665	10	Chl absorption
8	681.25	7.5	Fluorescence peak
9	708.75	10	Fluorescence; atm correction
10	753.75	7.5	Vegetation and clouds
11	760.625	3.75	O2 absorption band
12	778.75	15	Atm. Correction
13	865	20	vegetation and water vapor
14	885	10	Atm correction
15	900	10	Water vapor and land

A4. OLCI band characteristics from section 2.4

Band Number	Band Center (nm)	Band Width (nm)	Application
1	400	15	Aerosols
2	412.5	10	Yellow substance
3	442.5	10	Chl-a absorption max
4	490	10	Chl-a other pigments
5	510	10	Sediments, red tide
6	560	10	Chl-a absorption minimum
7	620	10	Sediment loading
8	665	10	Chl-a absorption, sediment
9	673.75	7.5	Chl-a fluorescence baseline
10	681.25	7.5	Chl-a fluorescence
11	708.75	10	Chl-a fluorescence baseline
12	753.75	7.5	O2 absorption

13	761.25	2.5	Aerosol correction
14	764.375	3.75	Atm correction
15	767.5	2.5	Cloud detection
16	778.75	15	Atm correction
17	865	20	Atm correction
18	885	10	Water vapor
19	900	10	Water vapor
20	940	20	Water vapor
21	1020	40	Atm aerosol correction

A5. Landsat-8 OLI specifications from section 2.6

Spectral Band	Wavelength (nm)	Spatial Resolution (m)	Application
1	433-453	30	chlorophyll, aerosol detection
2	450 – 515	30	Water color, chlorophyll, turbidity
3	525 – 600	30	Peak water reflectance, suspended material
4	630 – 680	30	Chl absorption, vegetation
5	845 – 885	30	Land water mask, vegetation
6	1560 – 1660	30	Atmospheric correction
7	2100 – 2300	30	Cloud land separation
8	500 - 680	15	Pan-sharpening
9	1360 – 1390	30	This cloud detection

A6. MSI band characteristics from Section 2.5

Band	Central Wavelength (nm)	Spatial Resolution (nm)	Bandwidth (nm)	Application
1	443	60	20	Aerosol, coastal water
2	490	10	65	Bathymetry, composites
3	560	10	35	Vegetation, suspended matter
4	665	10	30	Chl
5	705	20	15	Chl
6	740	20	15	Chl
7	783	20	20	Canopy discrimination
8	842	10	115	Vegetation indexes
8A	865	20	20	Bidirectional reflectance distribution function
9	945	60	20	Water vapor detection
10	1375	60	20	Cloud detection
11	1610	20	90	Cloud detection
12	2190	20	180	Minerology, moisture gradients

A7. VIIRS band characteristics from Section 2.7

VIIRS Band	Central λ (nm)	λ range (nm)	Primary Uses	Spatial Resolution (m)

M1	412	402-422	Pigment detection	750
M2	445	436-454	Pigment detection	750
M3	488	478-488	Pigment detection	750
M4	555	545-565	Pigment detection	750
M5(B)	672	662-682	Pigment detection	750
M6	746	739-754	Atm correction	750
M7(G)	865	846-885	Atm correction	750
M8	1240	1230-1250	Atm correction	750
M9	1378	1371-1386	Atm correction	750
M10	1610	1580-1640	Atm correction	750
M11	2250	2230-2280	Atm correction	750
M12	3700	3610-3790	Atm correction	750
M13	4050	3970-4130	Atm correction	750
M14	8550	8400-8700	Atm correction	750
M15	10763	10260-11260	Atm correction	750
M16	12013	11540-12490	Atm correction	750

A8. PACE band characteristics from Section 2.8

Band Number	Central Wavelength (nm)	Bandwidth (nm)
1	400	5 ± 0.5
2	405	5 ± 0.5
3	410	5 ± 0.5
4	415	5 ± 0.5
5	420	5 ± 0.5
6	425	5 ± 0.5
7	430	5 ± 0.5
8	435	5 ± 0.5
9	440	5 ± 0.5
10	445	5 ± 0.5
11	450	5 ± 0.5
12	455	5 ± 0.5
13	460	5 ± 0.5
14	465	5 ± 0.5

15	470	5 ± 0.5
16	475	5 ± 0.5
17	480	5 ± 0.5
18	485	5 ± 0.5
19	490	5 ± 0.5
20	495	5 ± 0.5
21	500	5 ± 0.5
22	505	5 ± 0.5
23	510	5 ± 0.5
24	515	5 ± 0.5
25	520	5 ± 0.5
26	525	5 ± 0.5
27	530	5 ± 0.5
28	535	5 ± 0.5
29	540	5 ± 0.5
30	545	5 ± 0.5
31	550	5 ± 0.5
32	555	5 ± 0.5
33	560	5 ± 0.5
34	565	5 ± 0.5
35	570	5 ± 0.5
36	575	5 ± 0.5
37	580	5 ± 0.5
38	586	5 ± 0.5
39	615	5 ± 0.5
40	620	5 ± 0.5
41	625	5 ± 0.5
42	630	5 ± 0.5
43	635	5 ± 0.5
44	640	5 ± 0.5
45	642	5 ± 0.5
46	645	5 ± 0.5
47	647	5 ± 0.5

48	650	5 ± 0.5
49	652	5 ± 0.5
50	655	5 ± 0.5
51	657	5 ± 0.5
52	660	5 ± 0.5
53	662	5 ± 0.5
54	665	5 ± 0.5
55	667	5 ± 0.5
56	670	5 ± 0.5
57	672	5 ± 0.5
58	675	5 ± 0.5
59	677	5 ± 0.5
60	679	5 ± 0.5
61	682	5 ± 0.5
62	697	5 ± 0.5
63	699	5 ± 0.5
64	702	5 ± 0.5
65	704	5 ± 0.5
66	707	5 ± 0.5
67	709	5 ± 0.5
68	712	5 ± 0.5
69	714	5 ± 0.5
70	719	5 ± 0.5
71	724	5 ± 0.5
72	729	5 ± 0.5
73	734	5 ± 0.5
74	739	5 ± 0.5
75	742	5 ± 0.5
76	744	5 ± 0.5
77	747	5 ± 0.5
78	749	5 ± 0.5
79	752	5 ± 0.5
80	754	5 ± 0.5

81	772	5 ± 0.5
82	774	5 ± 0.5
83	779	5 ± 0.5
84	784	5 ± 0.5
85	789	5 ± 0.5
86	794	5 ± 0.5
87	799	5 ± 0.5
88	804	5 ± 0.5
89	809	5 ± 0.5
90	814	5 ± 0.5
91	819	5 ± 0.5
92	824	5 ± 0.5
93	829	5 ± 0.5
94	835	5 ± 0.5
95	840	5 ± 0.5
96	845	5 ± 0.5
97	850	5 ± 0.5
98	855	5 ± 0.5
99	860	5 ± 0.5
100	865	5 ± 0.5
101	870	5 ± 0.5
102	875	5 ± 0.5
103	880	5 ± 0.5
104	885	5 ± 0.5
105	890	5 ± 0.5
106	895	5 ± 0.5
107	1038	75 ± 10
108	1249	30 ± 4
109	1618	75 ± 10
110	2131	50 ± 5
111	2258	75 ± 5

Appendix B: Flags

B1. SeaWiFS flags

Sensor-Seawifs	
Mask	Python Implementation

Cloud Mask (v1.0)	# load numpy arrays from SAPS L3 file
	cldalb = l3_file.get_data("cloud_albedo")
	chl = l3_file.get_data("chl_ocx")
	rrs_red = l3_file.get_data("Rrs_670")
	rhos_443 = l3_file.get_data("rhos_443")
	rhos_555 = l3_file.get_data("rhos_555")
	rhos_670 = l3_file.get_data("rhos_670")
	rhos_865 = l3_file.get_data("rhos_865")
	
	# First correct for turbid water
	numreal = rrs_red.copy()
	numreal[(chl >= 0)] = rrs_red[(chl >= 0)] * (0.45 + chl[(chl >= 0)] * 0.005) / 4.3
	numreal[(rrs_red < 0)] = 0
	
	# Need to capture nan's
	numreal[np.isnan(numreal)] = 0
	
	# create cloud mask and set all pixels equal 0
	cld = np.zeros(cldalb.shape, dtype=np.uint8)
	cld[(cldalb - numreal) > 0.027] = 1

Mixed/Invalid Pixel Mask (v0.1)	mixed_pixel = np.zeros(rhos_443.shape) mixed_pixel[(rhos_865 > rhos_443) & (rhos_865 > rhos_555) & (rhos_865 > rhos_670) & (rhos_865 > 0.01)] = 1

B2. MERIS/OLCI flags

Sensor-MERIS/OLCI	
Mask	Python Implementation

Cloud Mask (v1.3)	# load numpy arrays from SAPS L3 file
	cldalb = l3_file.get_data("cloud_albedo")
	rhos_442 = l3_file.get_data("rhos_442")
	rhos_490 = l3_file.get_data("rhos_490")
	rhos_560 = l3_file.get_data("rhos_560")
	rhos_620 = l3_file.get_data("rhos_620")
	rhos_665 = l3_file.get_data("rhos_665")
	rhos_681 = l3_file.get_data("rhos_681")
	rhos_709 = l3_file.get_data("rhos_709")
	rhos_754 = l3_file.get_data("rhos_754")
	rhos_865 = l3_file.get_data("rhos_865")
	rhos_885 = l3_file.get_data("rhos_885")
	
	# turbidity signal in water
	numreal = (rhos_620 + rhos_665 + rhos_681) - 3.0 * rhos_442 - (rhos_754 - rhos_442) / (754 - 442) * (620 + 665 + 681 - 3.0 *442)
	idx = (numreal > 0)
	cldtmp = cldalb.copy()
	
	# switch to rhos_865 where cldalb fails
	cldtmp[(np.isnan(cldalb))] = rhos_865[(np.isnan(cldalb))]
	cldtmp[idx] = cldalb[idx] - 3 * numreal[idx]
	
	# create cloud mask and set all pixels equal 0
	cld = np.zeros(cldalb.shape, dtype=np.uint8)
	
	cld[cldtmp > 0.08] = 1

Cloud Mask (Scum)	# to deal with scum look at relative of NIR and blue for lower albedos cld[((rhos_754 + rhos_709) > (rhos_443 + rhos_490)) & (cldalb < 0.1)] = 0 cld[((rhos_754 + rhos_709) - (rhos_665 + rhos_681) > 0.01) & (cldtmp < 0.15)] = 0 cld[(((rhos_754 + rhos_709) - (rhos_665 + rhos_681)) / cldtmp) > 0.1] = 0 cld[(rhos_665 > 0.1) & (cldalb > 0.15)] = 1

Cloud Mask (Glint)	# flag high glint cld[(rhos_865 - cldalb) > 0.25] = 1
Mixed Pixel Mask (v1.1)	# original test conditions: mixed_pixel[((rhos_885 > rhos_620) & (rhos_885 > rhos_709) & (rhos_885 > rhos_754) & (rhos_885 > 0.01))] = 1
Mixed Pixel Mask (dry lake)	# test dry lake condition: mixed_pixel[((rhos_620 > rhos_560) & (rhos_560 > 0.15) & (rhos_885 > 0.15))] = 1

Mixed Pixel Mask (snow/ice)	# test snow/ice condition:
	# MERIS differential snow index
	mdsi = (rhos_865 - rhos_885) / (rhos_865 + rhos_885)
	
	# exclude potential bloom conditions (use coefficient of variation in visible bands)
	cv = (np.nanstd(np.array([rhos_443, rhos_490, rhos_510, rhos_560, rhos_620, rhos_665, rhos_681]), axis=0) / np.nanmean(np.array([rhos_443, rhos_490, rhos_510, rhos_560, rhos_620, rhos_665, rhos_681]), axis=0))
	
	mixed_pixel[((mdsi > 0.01) & (rhos_885 > 0.15) & (cv < 0.1))] = 1

Adjacency Mask (v1.0)	ci = calc_ci(rhos_665, rhos_681, rhos_709)
	ci = apply_kd_corr(ci, rhos_442, rhos_490, rhos_510, rhos_560, rhos_620, rhos_665, rhos_709, rhos_865)
	
	mci =calc_mci(rhos_681, rhos_709, rhos_754)
	
	# create mask and set all pixels equal 0
	mask = np.zeros(rhos_490.shape, dtype=np.uint8)
	
	# flag adjacency pixels
	adj_mask[((ci>0) & (mci<0))] = 1

B3. MODIS flags

Sensor-MODIS	
Mask	Python Implementation

Cloud Mask (v1.2)	# load numpy arrays from SAPS L3 file
	cldalb = l3_file.get_data("cloud_albedo")
	rhos_469 = l3_file.get_data("rhos_469")
	rhos_555 = l3_file.get_data("rhos_555")
	rhos_645 = l3_file.get_data("rhos_645")
	rhos_859 = l3_file.get_data("rhos_859")
	rhos_1240 = l3_file.get_data("rhos_1240")
	rhos_2130 = l3_file.get_data("rhos_2130")
	
	numreal = rrs_red.copy()
	idx = (chl >= 0)
	numreal[idx] = rrs_red[idx] * (0.45 + chl[idx] * 0.005) / 4.3
	
	# first correct for turbid water
	numreal[rrs_red < 0] = 0
	
	# need to capture nan pixels
	numreal[np.isnan(numreal)] = 0
	
	# create cloud mask and set all pixels equal 0
	cld = np.zeros(cldalb.shape, dtype=np.uint8)
	# switch to rhos_859 where cldalb fails
	cldalb[(np.isnan(cldalb))] = rhos_859[(np.isnan(cldalb))]
	cld[(cldalb - numreal) > 0.027] = 1

Cloud Mask (Non-Water Check)	# non-water check 1240 is bright relative to 859 & the combination is bright # this may hit glint by accident, need to be checked. cld[((rhos_1240 / rhos_859 > 0.5) & (rhos_1240 + rhos_2130 > 0.10))] = 1

Cloud Mask (Glint)	# now try to correct for glint
	numreal = rhos_645 - rhos_555 + (rhos_555 - rhos_859) * (645 - 555) / (859 - 555)

	# need to capture nan pixels numreal[np.isnan(numreal)] = 0 numreal_1 = cldalb + numreal [((cldalb > 0) & (numreal_1 < 0.027))] = 0 cld[(rhos_859 / rhos_1240 > 4)] = 0
Cloud Mask (Scum)	# scum areas cld[((rhos_859 - rhos_469 > 0.02) & (cldalb > 0) & (cldalb < 0.30))] = 0 cld[((rhos_859 - rhos_645 > 0.01) & (cldalb > 0) & (cldalb < 0.30))] = 0 idx = (rhos_1240 < 0.2) numreal_1[idx] = (numreal_1[idx] - (rhos_859[idx] - rhos_1240[idx]) * np.abs(rhos_859[idx] - rhos_1240[idx]) / 0.027)

Cloud Mask (water areas)	# water areas
	numreal_2 = numreal_1.copy()
	idx = ((numreal_1 < 0.027 * 2) & ((rhos_555 - rhos_1240) > (rhos_469 - rhos_1240)))
	numreal_2[idx] = numreal_1[idx] - (rhos_555[idx] - rhos_1240[idx])
	idx = ((numreal_1 < 0.027 * 2) & ((rhos_555 - rhos_1240) <= (rhos_469 - rhos_1240)))
	numreal_2[idx] = numreal_1[idx] - (rhos_469[idx] - rhos_1240[idx])
	
	cld[(cldalb > 0) & (numreal_2 < 0.027)] = 0
	# force cloud
	# - exclude potential bloom conditions (use coefficient
	# of variation in visible bands)
	cv = (np.std(np.array([rhos_469, rhos_555, rhos_645]), axis=0) /
	np.mean(np.array([rhos_469, rhos_555, rhos_645]), axis=0))
	cld[((cldalb > 0.12) & (cv < 0.12))] = 1

Cloud Mask (Glint)	#flag high glint cld[(rhos_859 - cldalb) > 0.25] = 1

Mixed Pixel Mask (v1.1)	mixed_pixel = np.zeros(rhos_469.shape)
	# normalized difference flood index
	ndfi =(rhos_645 - rhos_2130) / (rhos_645 + rhos_2130)
	
	if l3_file.bands_in_file(['rhos_678']):
	  rhos_678 = l3_file.get_data('rhos_678', min_val=self.min_rhos, max_val=self.max_rhos)
	  mixed_pixel[(rhos_859 > rhos_469) & (rhos_859 > rhos_555) & (rhos_859 > rhos_645) & ((rhos_1240 > rhos_645) | (rhos_1240 > rhos_678) | (ndfi < 0.6)) & (rhos_859 > 0.01) & ((rhos_2130 > 0.015) | (ndfi < 0.6))] = 1
	else:
	  #hmodis L3's do not include rhos_678 so use alternate masking
	  mixed_pixel[(rhos_859 > rhos_469) & (rhos_859 > rhos_555) & (rhos_859 > rhos_645) & ((rhos_1240 > rhos_645) | (ndfi < 0.6)) & (rhos_859 > 0.01) & ((rhos_2130 > 0.015) | (ndfi < 0.6))] = 1
	
	mixed_pixel[(rhos_1240 > rhos_555) & (rhos_1240 < 0.1)] = 1

B4. MSI flags

Sensor-MSI (L2 processed using SNAP GPT RayleighCorrection)	
Mask	Python Implementation
Cloud Mask (v1.2)	# Bottom of Rayleigh Reflectance band names (rBRR) are mapped to equivalent rhos gpt_rhos2BRR('rhos_443': 'rBRR_B1', 'rhos_492': 'rBRR_B2', 'rhos_560': 'rBRR_B3', 'rhos_665': 'rBRR_B4', 'rhos_704': 'rBRR_B5', 'rhos_740': 'rBRR_B6', 'rhos_783': 'rBRR_B7', 'rhos_835': 'rBRR_B8', 'rhos_865': 'rBRR_B8A', 'rhos_945': 'rBRR_B9', 'rhos_1613': 'rBRR_B11',

	'rhos_2200': 'rBRR_B12')
	
	# load numpy arrays from SAPS L3 file
	rhos_443 = l3_file.get_data(gpt_rhos2BRR("rhos_443"))
	rhos_492 = l3_file.get_data(gpt_rhos2BRR("rhos_492"))
	rhos_560 = l3_file.get_data(gpt_rhos2BRR("rhos_560"))
	rhos_665 = l3_file.get_data(gpt_rhos2BRR("rhos_665"))
	rhos_704 = l3_file.get_data(gpt_rhos2BRR("rhos_704"))
	rhos_740 = l3_file.get_data(gpt_rhos2BRR("rhos_740"))
	rhos_865 = l3_file.get_data(gpt_rhos2BRR("rhos_865"))
	cldalb = rhos_865
	numreal = rhos_665 - rhos_443 - (rhos_740 - rhos_443) / (740 - 443) * (665 - 443)
	
	idx = (numreal > 0)
	cldtmp = cldalb.copy()
	
	# switch to rhos_865 where cldalb fails
	cldtmp[(np.isnan(cldalb))] = rhos_865[(np.isnan(cldalb))]
	cldtmp[idx] = cldalb[idx] - 3 * numreal[idx]
	
	#create cloud mask and set all pixels equal 0
	cld = np.zeros(cldalb.shape, dtype=np.uint8)
	
	cld[cldtmp > 0.08] = 1

Cloud Mask (Scum)	# to deal with scum look at relative of NIR and blue for lower albedos cld[((rhos_740 + rhos_704) > (rhos_443 + rhos_492)) & (cldtmp < 0.1) & (rhos_560 > rhos_665)] = 0 # no rhos_681, so replace with rhos_665 cld[((rhos_740 + rhos_704) - (rhos_665 + rhos_665) > 0.01) & (cldtmp < 0.15) & (rhos_560 > rhos_665)] = 0 cld[((((rhos_740 + rhos_704) - (rhos_665 + rhos_665)) / cldtmp) > 0.1) & (rhos_560 > rhos_665)] = 0

	cld[(rhos_665 > 0.1) & (cldtmp > 0.15)] = 1
Cloud Mask (Glint)	# flag high glint cld[(rhos_865 - cldalb) > 0.25] = 1
Mixed Pixel Mask (v1.0)	mixed_pixel = np.zeros(rhos_665.shape) # original test conditions: mixed_pixel[((rhos_865 > rhos_665) & (rhos_865 > rhos_704) & (rhos_865 > rhos_740) & (rhos_865 > 0.01))] = 1
Mixed Pixel Mask (dry lake)	# test dry lake condition: mixed_pixel[((rhos_665 > rhos_560) & (rhos_560 > 0.15) & (rhos_865 > 0.15))] = 1

Appendix C: Clear water correction

CI: MODIS clear water correction

Sensor-MODIS	
Threshold	Python Implementation

0.51	#calculate standard Kd for correction
	kd =calc_kd_rhos(rhos_469, rhos_645, rhos_859)
	
	#expect a 560 peak with cyano blooms
	ss_555 = (rhos_555 - rhos_469 + (rhos_469 - rhos_645) * (555 - 469) / (645 - 469))
	
	ci[(kd < kd_min_threshold) & ((rhos_859 <= rhos_469) | (rhos_859 <= rhos_645)) & (ss_555 < 0.01)] = 0

C2: MERIS/OLCI clear water correction

Sensor-MERIS/OLCI	
Threshold	Python Implementation
0.31	def calc_kd_rhos(self, rhos_442, rhos_490, rhos_620, rhos_665, rhos_885): """Kd calculation with 885 correction applied.""" kd = 0.7 * ((((rhos_620 + rhos_665) / 2.0) - rhos_885) / (((rhos_442 + rhos_490) / 2.0) - rhos_885)) # mask overcorrected pixels kd[((((rhos_620 + rhos_665) / 2.0) - rhos_885) < 0) | ((((rhos_442 + rhos_490) / 2.0) - rhos_885) < 0)] = np.nan return kd

	# calculate standard Kd for correction
	kd = calc_kd_rhos(rhos_442, rhos_490, rhos_620, rhos_665, rhos_865)
	
	# calculate Kd using rhos_709 instead of rhos_620 & rhos_665
	kd_709 = calc_kd_rhos(rhos_442, rhos_490, rhos_620, rhos_709, rhos_865)
	# 709 switching modification for scum conditions
	kd[(kd_709 > kd)] = kd_709[(kd_709 > kd)]
	
	# expect a 560 peak with cyano blooms
	ss_560 = (rhos_560 - rhos_442 + (rhos_442 - rhos_620) * (560 - 442) / (620 - 442))
	
	# set CI pixels identified as clearwater to 0
	ci[(kd < self.kd_min_threshold) & ((rhos_865 <= rhos_490) | (rhos_865 <= rhos_665) |
	(rhos_865 <= rhos_709)) & (ss_560 < 0.01)] = 0
	# if no valid Kd and rhos_885 very low assume clearwater
	ci[np.isnan(kd) & (rhos_885 < 0.005)] = 0

Appendix D: High turbidity correction

OLCI/MERIS turbidity correction

Sensor-MERIS/OLCI
Python Implementation

#calculate SS620
ss620 = rhos_620 - rhos_560 + (rhos_560 - rhos_665) * (620-560) / (665-560)
ci[(ss620 > 0)] | (rhos_560 < rhos_620)] = 0

Appendix E: Scaling Factors

Scaling factors are needed to go from a geophysical value (such as Chl-*a* concentration in µg Level 1) to a scaled number from 0-250 for an output product (Level 2+). Additionally, the scaling factor can be seen in the metadata from each product using the gdal utility found in Appendix G (gdalinfo <ProductName*.tif> | grep "SAPS"). Use the un-scaling equation to convert from the scaled number (DN) to the geophysical value.

Product	Scaling	Un-scaling
CI	Scaled = (83.3)*(Log_{10}(CI + 4.2))	$Unscaled = 10^{(3.0 / 250.0 * DN - 4.2)}$
MCI	Scaled = (250 / 3)*(4 + Log_{10} (MCI))	$Unscaled = 10^{(0.012 * DN - 4)}$
Chl (coastal)	Scaled = (275 / (1 + 13.46374 / chl))	Unscaled = 13.46374 / ((275.0 / DN) - 1)
Chl (global)	Scaled = (250.0 / 3.0) * (1.3 + Log_{10} (chl))	$Unscaled = 10^{(0.012 * DN - 1.3)}$
K_d	Scaled = 325 / (1 + 2.71828 / K_d)	Unscaled = 2.71828 / ((325.0 / DN) - 1)
R_{rs}	Scaled = (270 / (1+0.00609675 / Rrs665))	Unscaled = 0.00609675 / ((270.0 / DN) - 1)
RBD	Scaled = 150 * (4 + Log_{10} (RBD))	$Unscaled = 10^{(DN / 150. - 4)}$

Appendix F: SAPS script listing

S.N.	Script	Description
1	create_metadata.py	Create metadata file for a list of SAPS products
2	create_saps_colorbars.py	Add colorbar to SAPS product or create standalone colorbar for product
3	get_sentinel_data.py	Search for and download S3 OLCI or S2 MSI data
4	get_nasa_data.py	Search and download OLCI, MERIS, MODIS, PACE data
5	run_compare_products.py	Utility module to compare SAPS products
6	run_daily_nrt_modis.py	Run MODIS daily near real-time processing
7	run_daily_nrt_olci.py	Run OLCI daily near real-time processing
8	run_olci_reprocess.py	Reprocess OLCI using non-time critical L1B inputs
9	run_modis_reprocess.py	Reprocess MODIS with refined ancillary and calibration inputs
10	run_make_custom_products.py	Test and run custom products from SAPS L3 files
11	run_make_products.py	Creates products from SAPS L3 files

12	run_make_default_products.py	Create default products based on SAPS area config file
13	run_saps_file_info.py	Display internal SAPS product metadata
14	saps_azure_upload.py	Upload products to Azure storage
15	atlas_azure_upload.py	Upload products to Azure storage from Atlas
16	saps_get_modis.py	Download MODIS L0 data
17	saps_make_area_landmask.py	Utility module to create a SAPS landmask
18	saps_ngs_upload.py	Upload products via FTP
19	saps_processor.py	Run all processing steps to generate both SAPS L3 and product files for list of input files
20	saps_show_products.py	Utility module to display information about product algorithms
21	saps_zonal_stats.py	Utility module to generate zonal statistics
22	swap_colortable.py	Utility module to replace color table in SAPS GeoTiFF product
23	saps_setup_env	Define command line environment to run SAPS modules

Appendix G: Processing flowcharts

F1. MODIS processing flowchart

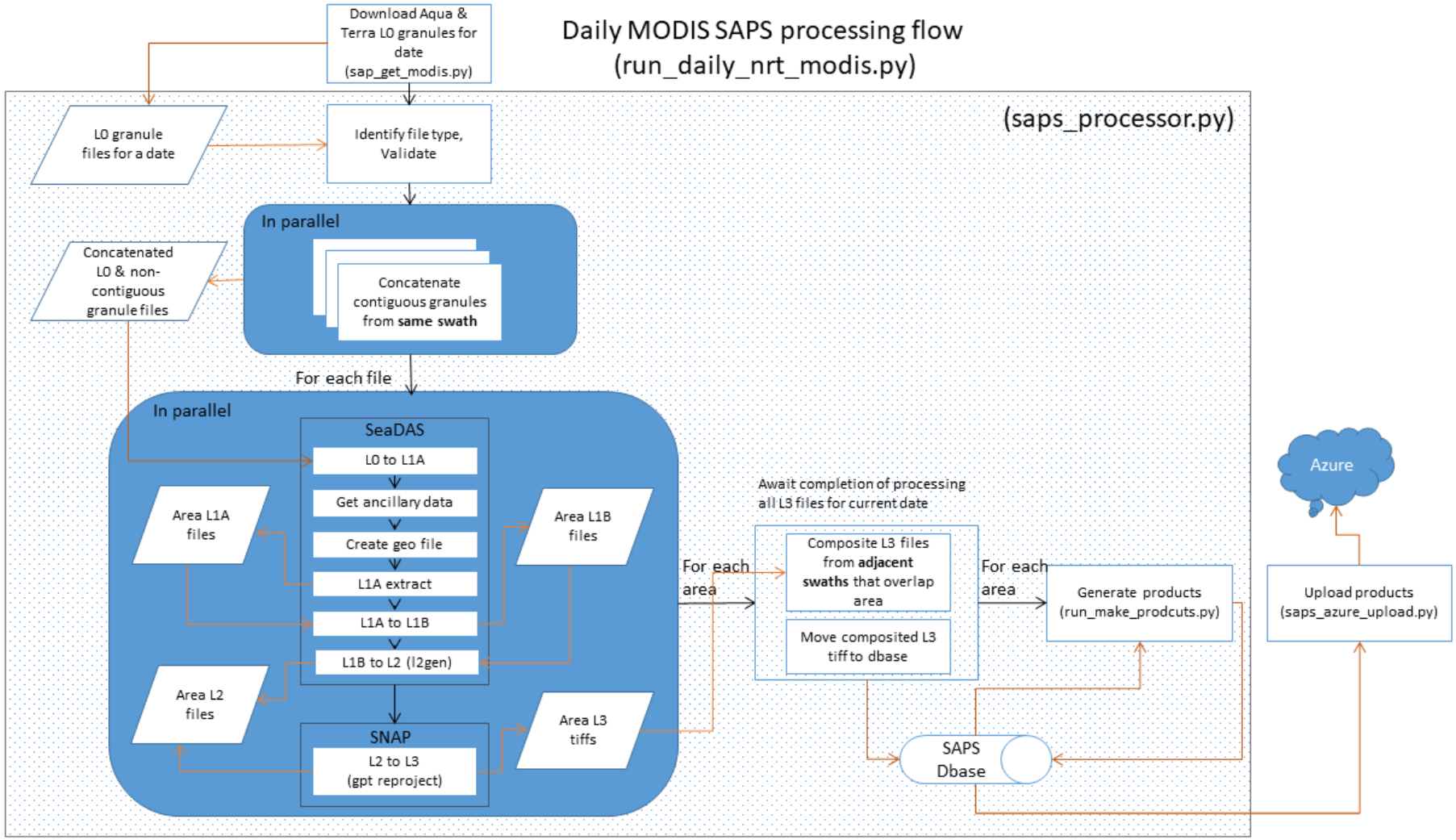
Daily MODIS SAPS processing flow
(run_daily_nrt_modis.py)
(saps_processor.py)
Download Aqua & Terra L0 granules for date (sap_get_modis.py)
L0 granule files for a date
Identify file type, Validate
In parallel
Concatenated L0 & non-contiguous granule files
Concatenate contiguous granules from same swath
For each file
In parallel
SeaDAS
L0 to L1A
Get ancillary data
Create geo file
L1A extract
L1A to L1B
L1B to L2 (l2gen)
Area L1A files
Area L1B files
Area L2 files
SNAP
L2 to L3 (gpt reproject)
Area L3 tiffs
For each area
Await completion of processing all L3 files for current date
Composite L3 files from adjacent swaths that overlap area
Move composited L3 tiff to dbase
For each area
Generate products (run_make_prodcuts.py)
SAPS Dbase
Azure
Upload products (saps_azure_upload.py)

F2. OLCI processing flowchart

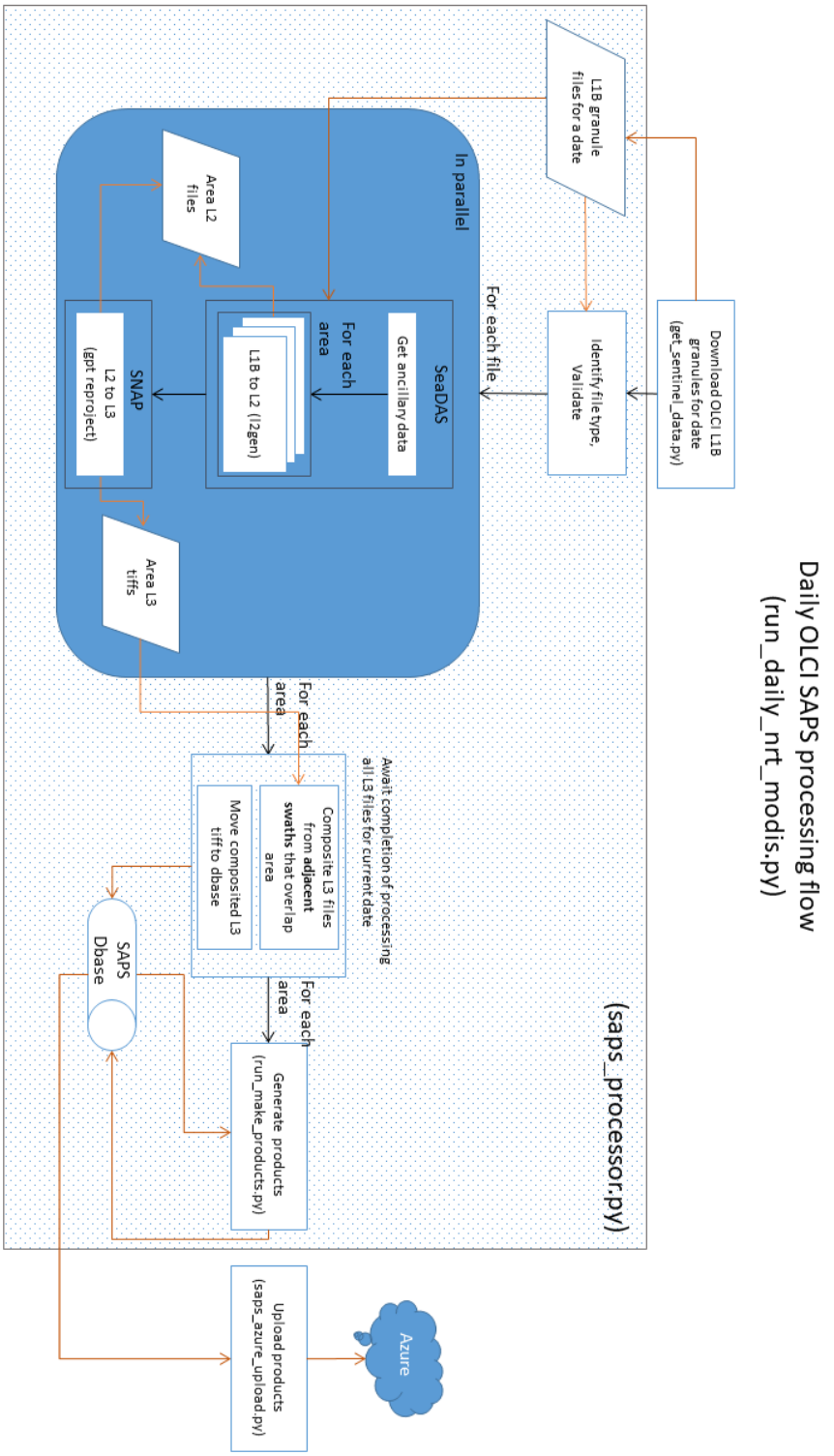

Appendix H: Sample metadata extract

The *gdalinfo* utility distributed as part of the gdal open-source software package (https://gdal.org/) can be used to view internal metadata within SAPS GeoTiff products. Here is an example of running the command in a Linux terminal window to display the SAPS specific metadata from the envisat.2003364.1230.1844C.L3.CAN.v670_1_2.rrs665.tif product located in the currently directory:
gdalinfo envisat.2003364.1230.1844C.L3.CAN.v670_1_2.rrs665.tif | grep "SAPS"

Command output:

```
SAPS_cloud_mask_desc=Meris SAPS cloud mask
SAPS_cloud_mask_name=meris_cloud
SAPS_cloud_mask_version=1.1
SAPS_mixed_pixel_mask_desc=Meris mixed pixel mask
SAPS_mixed_pixel_mask_name=meris_mixpix
SAPS_mixed_pixel_mask_version=1.1
SAPS_nodata_mask_desc=No data coverage mask
SAPS_nodata_mask_name=nodata
SAPS_nodata_mask_version=1.0
SAPS_product_created=20180905T0835
SAPS_product_desc=Turbidity based on rrs_665
SAPS_product_flag_cloud=253
SAPS_product_flag_invalid=254
SAPS_product_flag_land=252
SAPS_product_flag_nodata=255
SAPS_product_flag_nodetect=0
SAPS_product_flag_saturated=250
SAPS_product_lut_fn=viridis_red_v2.txt
SAPS_product_masking=CMDL
SAPS_product_name=rrs665
SAPS_product_rev_scaling=0.00609675 / ((270.0 / DN) - 1)
SAPS_product_scaling=np.round(270 / (1 + 0.00609675 / rrs_665[rrs_665>0]))
SAPS_product_src=envisat.2003364.1230.1844C.L3.CAN.v670_1.tif
SAPS_product_type=standard_prod
SAPS_product_version=1.0
```

Below is an example of the metadata from a SAPS CI GeoTiFF file:
SAPS info:

```
SAPS_ci_adj_mask_desc = SAPS CI adjacency mask based on CI detect and no MCI detect
SAPS_ci_adj_mask_name = ci_adj
SAPS_ci_adj_mask_version = 1.0
SAPS_cloud_mask_desc = OLCI SAPS cloud mask
```

SAPS_cloud_mask_name = olci_cloud
SAPS_cloud_mask_version = 1.0
SAPS_mixed_pixel_mask_desc = OLCI mixed pixel mask
SAPS_mixed_pixel_mask_name = olci_mixpix
SAPS_mixed_pixel_mask_version = 1.1
SAPS_nodata_mask_desc = No data coverage mask
SAPS_nodata_mask_name = nodata
SAPS_nodata_mask_version = 1.0
SAPS_product_created = 20180417T1106
SAPS_product_desc = Chlorophyll Cyanobacteria Index with Kd clear water correction and CInoMCI adjacency flagging
SAPS_product_flag_adjacency = 251
SAPS_product_flag_cloud = 253
SAPS_product_flag_invalid = 254
SAPS_product_flag_land = 252
SAPS_product_flag_nodata = 255
SAPS_product_flag_nodetect = 0
SAPS_product_flag_saturated = 250
SAPS_product_lut_fn = viridis_red_v2.txt
SAPS_product_masking = CMADL
SAPS_product_name = CI
SAPS_product_rev_scaling = 10**(3.0 / 250.0 * DN - 4.2)
SAPS_product_scaling = np.round(83.3 * (np.log10(ci[ci>0]) + 4.2))
SAPS_product_src = sentinel-3a.2017220.0808.1526_1527C.L3.OH3.v8103_1.tif
SAPS_product_type = standard_prod
SAPS_product_version = 1.1

U.S. Department of Commerce
National Oceanic and Atmospheric Administration
National Ocean Service
National Centers for Coastal Ocean Science
Harmful Algal Bloom Forecasting Branch

The National Centers for Coastal Ocean Science delivers ecosystem science solutions for stewardship of the nation's ocean and coastal resources in direct support of National Ocean Service (NOS) priorities, offices, and customers to sustain thriving coastal communities and economies. For more information, visit: http://www.coastalscience.noaa.gov/